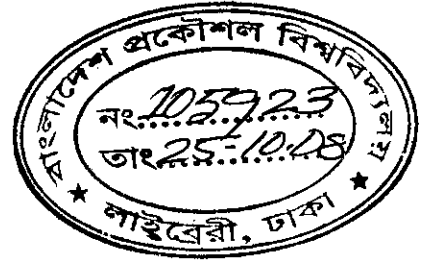


Optimum Channel Shortening for Cyclic Prefixed Multicarrier Communication Systems

by



Toufiqul Islam

MASTER OF SCIENCE IN ELECTRICAL AND ELECTRONIC ENGINEERING



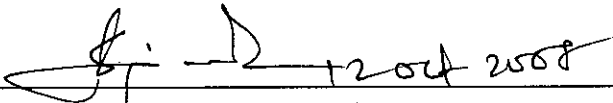
#105923#

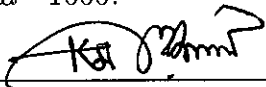
DEPARTMENT OF ELECTRICAL AND ELECTRONIC ENGINEERING
BANGLADESH UNIVERSITY OF ENGINEERING AND TECHNOLOGY

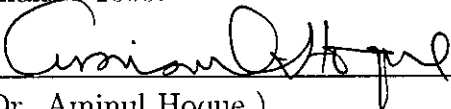
October 2008

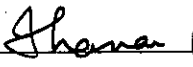
The thesis entitled "Optimum Channel Shortening for Cyclic Prefixed Multicarrier Communication Systems" submitted by Toufiqul Islam Roll No.: 100606237P, Session: October, 2006 has been accepted as satisfactory in partial fulfillment of the requirements for the degree of Master of Science in Electrical and Electronic Engineering on October 12, 2008.

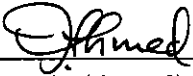
BOARD OF EXAMINERS

1. 

(Dr. Satya Nrasad Majumder)
Professor
Department of Electrical and Electronic Engineering
Bangladesh University of Engineering and Technology
Dhaka - 1000. **Chairman**
(Supervisor)
2. 

(Dr. Md. Kamrul Hasan)
Pro-Vice Chancellor
East West University, Dhaka - 1212.
Professor (On leave)
Department of Electrical and Electronic Engineering
Bangladesh University of Engineering and Technology
Dhaka - 1000. **Member**
(Co-supervisor)
3.  12/10/08

(Dr. Aminul Hoque)
Professor and Head
Department of Electrical and Electronic Engineering
Bangladesh University of Engineering and Technology
Dhaka - 1000. **Member**
(Ex-officio)
4.  12.10.08

(Dr. Mohammed Imamul Hassan Bhuiyan)
Assistant Professor
Department of Electrical and Electronic Engineering
Bangladesh University of Engineering and Technology
Dhaka - 1000. **Member**
(Internal)
5.  12.10.08

(Dr. Farruk Ahmed)
Professor
Department of Computer Science and Engineering
North South University, Dhaka - 1209. **Member**
(External)

Declaration

It is hereby declared that this thesis or any part of it has not been submitted elsewhere for the award of any degree or diploma.

Signature of the candidate



(Toufiqul Islam)

Dedication

To my beloved family.

Acknowledgements

During the course of my life I have come to realize that a man does not stand on his own as there always are those who care and who help along and without whose support nothing would be possible. This is especially true in my case.

First of all, I would like to thank and express sincere appreciation to my supervisor Prof. Dr. Satya Prasad Majumder for his important support and assistance for the completion of this research work. I am very much grateful to him as he agreed to be my supervisor in crucial phase of the thesis to guide the work to the end.

I express my gratitude to Prof. Dr. Md. Kamrul Hasan, my co-supervisor, for guiding me in my graduate research. My respect for him grew when I took his course on digital signal processing, EEE 403. He was always able to take a daunting and difficult to understand concept and simplify it and make it unintimidating. His success and emphasis on clearly expressing complicated ideas helped me a lot in writing papers and preparing presentations. What I like the most about him is his exacting attitude for reviewing the papers. He always wants to be perfectionist in review for quality judgement. He introduced me to writing papers and thesis in LaTeX. During most of the phases of the research work, he carefully supervised my work and helped me to gain insight in the complex but beautiful world of signal processing. He has my deepest respect professionally and personally.

I would like to thank Prof. Dr. Aminul Hoque, the Head of the EEE department, BUET, for his valuable suggestions and granting me permission to work in the DSP lab and computer room. High speed computing facilities provided by the department was a great boost in my thesis work.

I want to thank Dr. Md. I. H. Bhuiyan and Md. Ariful Haque for providing me valuable advices and tips on writing thesis in LaTeX. On many occasions,

I took help from them, sometimes in person sometimes over phone, for solving different problem for writing in LaTeX.

I like to express my gratitude to Prof. Dr. Farruk Ahmed for giving me time and opportunity to discuss my work with him. He also helped me by making me acquainted with common writing practices/style for thesis.

I also like to thank Dr. Rick Martin (AFIT, OH, USA), Prof. Brian L. Evans (UT Austin, TX, USA), Andre Tkacenko (JPL, NASA, CA, USA) and Shafi Al Bashar (UC Davis, CA, USA) for their valuable discussion on the topic of this work.

I want to express my deepest gratitude to my parents. Without their effort, I would not be here today. I am indebted to them for the sacrifices that they made to put me through school as an undergraduate. It is my hope that some day I will be able to be as good of a parent to my children as my parents have been to me. I would like to give a special thanks to my wife, Rubaiya. She came into my life when I least expected it and most needed it. She has been a light in my darkness and has shown me true happiness. I want to thank her for caring me and supporting me during this tumultuous time in my life.

Last, but certainly not least, I would like to thank Almighty *Allah*, the Infinite Being, for creating this beautiful world in which we all live and beautiful mathematics (some of which I will present here in my thesis) and most importantly, for arousing kindness in so many people who provided me with the necessary support I required. I also want to thank Him for always watching over me and protecting me (even when I did not deserve it). Whenever I put my faith in His will, He always led me on the right path. I pray that His love and divine presence will be with us all, now and ever, and unto the ages of ages. Ameen.

Contents

Acknowledgements	iv
List of abbreviations	ix
List of Figures	x
List of Tables	xiii
Abstract	xiv
1 Introduction	1
1.1 Channel shortening	1
1.2 Discrete multitone modulation	2
1.2.1 DMT transmitter	4
1.2.2 DMT receiver	5
1.3 Equalization for discrete multitone modulation	5
1.4 Objective of the thesis	7
1.5 Organization of this thesis	8
2 Eigenfilter based TEQ design methods: Literature survey	10
2.1 Introduction	10
2.2 Common TEQ design formulation	10
2.3 Single Rayleigh quotient cases	12
2.3.1 The Maximum Shortening SNR (MSSNR) method	12
2.3.2 The Minimum Mean Squared Error (MMSE) method	13
2.3.3 The Minimum Inter-Symbol Interference (Min-ISI) method	15
2.3.4 The Minimum Delay Spread (MDS) method	15
2.4 Shortcomings of reported eigenfilter methods	16

2.4.1	MSSNR method	16
2.4.2	MMSE method	18
2.4.3	Min-ISI method	19
2.4.4	MDS method	20
2.5	Conclusion	21
3	Development of optimum channel shortening algorithms	22
3.1	Introduction	22
3.2	System model	22
3.3	Noise optimized minimum delay spread TEQ design method	24
3.3.1	Problem formulation	25
3.3.2	Optimum TEQ design	27
3.3.3	Simulation results	28
3.4	Improved eigenfilter based TEQ design method	32
3.4.1	The EIGFILT method	33
3.4.2	Development of a new objective function	34
3.4.3	Optimum TEQ design	36
3.4.4	Heuristic choice of optimum Δ	37
3.4.5	Experimental results	38
3.5	Iterative MSSNR method	41
3.5.1	Modified MSSNR cost function	41
3.5.2	Development of iterative MSSNR design	42
3.5.3	Step size adaptation	43
3.5.4	Simulation results	44
3.6	Conclusion	48
4	The MIMO channel shortening algorithm	49
4.1	Introduction	49
4.2	System model	50
4.3	Proposed MIMO MSSNR channel shortening	51
4.3.1	Problem formulation	51
4.3.2	Optimum MIMO TEQ design	53
4.4	Simulation results	54
4.5	Conclusion	59

5 Conclusion	60
5.1 Summary	60
5.2 Suggestions for future work	62
References	64
A Analysis of important equations	69
A.1 Proof of equivalence of equation 4.12 and 4.13	69
A.2 Decomposition of generalized EV problem of equation 3.39	70
B Configuration of 8 CSA loop TP channels	71
C List of publications	73

List of abbreviations

CP	Cyclic Prefix
SNR	Signal to Noise Ratio
DMT	Discrete Multitone
FFT	Fast Fourier Transform
DFT	Discrete Fourier Transform
OFDM	Orthogonal Frequency Division Multiplexing
TEQ	Time Domain Equalizer
ISI	Inter Symbol Interference
ICI	Inter Carrier Interference
BER	Bit Error Rate
MSSNR	Maximum Shortening SNR
MMSE	Minimum Mean Square Error
MSE	Mean Square Error
MDS	Minimum Delay Spread
ADSL	Asymmetric Digital Subscriber Line
VDSL	Very-high-speed Digital Subscriber Lines
SINR	Signal to Interference plus Noise Ratio
SIR	Shortened Impulse Response
EV	Eigenvector
CIR	Channel Impulse Response
QoS	Quality of Service

List of Figures

- 1.1 Illustration of channel shortening with a receiver filter. Here, \mathbf{h} and \mathbf{w} denote channel and equalizer, respectively. 2
- 1.2 Channel Bandwidth and Multicarrier Modulation. DMT Modulation has subchannels that are 4.3125 kHz wide in ADSL [1]. 3
- 1.3 Block diagram of a multicarrier modulation system. N denotes (I)FFT size, B denotes channel frequency coefficients. 4
- 1.4 Illustration of OFDM spectrum. In each sample of FFT grid, one subcarrier has peak while others have nulls. 6

- 2.1 Decomposition of the effective channel $c(k)$ into a desired channel $c_{des}(k)$ and residual channel $c_{res}(k)$. Δ denotes transmission delay. 13
- 2.2 MMSE system model. The symbols \mathbf{h} , \mathbf{w} , and \mathbf{b} are the impulse responses of the channel, the TEQ, and the target, respectively. Here, Δ represents transmission delay. The dashed lines indicate a virtual path, which is used only for analysis. 14
- 2.3 Original and shortened channel by MSSNR method. TEQ length = 17, Channel length = 512, window length $\nu + 1 = 32$. Only first 200 samples are shown. 17
- 2.4 Magnitude response of original and shortened channel by MSSNR method. 17
- 2.5 Original and shortened channel by MMSE method. TEQ length = 17, Channel length = 512, window length $\nu + 1 = 32$. Only first 200 samples are shown. 18
- 2.6 Magnitude response of original and shortened channel by MMSE method. 19

2.7	Original and shortened channel by Min-ISI method. TEQ length = 17, Channel length = 512, window length $\nu + 1 = 32$. Only first 200 samples are shown.	20
2.8	Magnitude response of original and shortened channel by Min-ISI method.	20
2.9	Original and shortened channel by MDS method. TEQ length = 17, Channel length = 512. Only first 200 samples are shown.	21
3.1	System model with channel/equalizer.	23
3.2	Cost function J gradually stabilizes with iterations (for CSA loop 8).	28
3.3	Original and shortened channel impulse responses (for CSA loop 8).	29
3.4	Original and shortened channel frequency responses (for CSA loop 8).	29
3.5	Variation of the delay spread as function of TEQ length (for CSA loop 1).	30
3.6	Equalizer output SNR as function of TEQ length (for CSA loop 1).	31
3.7	Original and equalized channel impulse responses for CSA loop no. 1. Location of k_{ref} and Δ_{heu} are shown for that channel.	37
3.8	Illustration of heuristic delay Δ_{heu} .	38
3.9	Frequency response of original and equalized channel in (a) and bit allocation over subcarriers in (b) for TEQ designed by the method in [2] and the proposed method, respectively, for CSA loop no. 1.	39
3.10	Observed bit rate for CSA loops no. 1-8 using various TEQ design methods. From left to right, height of the bars for each CSA loop denote bit rate obtained by MMSE-UEC [3], MSSNR [4], MDS [5], eigenfilter [2], proposed method with and without Δ_{heu} , respectively.	40
3.11	Performance of iterative MSSNR algorithm for CSA loop no. 8. Two kinds of initialization used: a) random and b) impulse.	43
3.12	Shortened channel by iterative MSSNR algorithm for CSA loop no. 8 (for random initialization). Shortened channel using adaptive μ almost coincides with direct MSSNR solution.	45

3.13	Bit allocation in different subcarriers by iterative algorithm. It is clear that iterative algorithm allows more subcarriers to carry bits (for CSA loop no. 8).	46
3.14	Frequency response of the shortened channel. It is clear that iterative algorithm avoids severe nulls in the useful signal band (for CSA loop no. 7).	46
3.15	Bit allocation in different subcarriers by iterative algorithm. This figure supports Fig. 3.14 that how more subcarriers can be utilized by iterative method unlike direct MSSNR approach (for CSA loop no. 7).	47
4.1	MIMO TEQ model, for L transmit antennas and P receive antennas. Channel $h^{(n,l)}$ connects the l th transmitter to the p th receiver antenna. $y_k^{(j)}$ denotes k th sample of equalizer output at j th receive antenna.	50
4.2	Variation of the equalization SNR of the MIMO TEQ vs delay over 100 channel realizations ($p = 7, q = 12, \nu = 2, L = 2, P = 2$).	56
4.3	Variation of the equalization SNR as a function of TEQ length.	56
4.4	Energy Compaction ratio as a function of TEQ length.	57
4.5	Variation of the SINR as a function of TEQ length.	57
4.6	Original and shortened channels($p = 300, q = 13, \nu = 15, L = 2, P = 2$) (MSSNR method).	58
4.7	Original and shortened channels($p = 300, q = 13, \nu = 15, L = 2, P = 2$) (MMSE method).	58
B.1	Configuration of eight standard CSA loops. Numbers represent length/thickness in feet per gauge. Vertical lines represent bridge taps.	72

List of Tables

3.1	Channel shortening notation	23
3.2	Observed delay spread for various methods (averaged over eight CSA loops)	31
3.3	Output SNR (in dB) comparison of various delay spread minimizing methods	31
3.4	Bit rate comparison with [6]	32
3.5	Shortening SNR comparison for direct and iterative MSSNR methods. All values in dB.	45
3.6	Bit rate comparison for direct and iterative MSSNR methods. All values in Mbps.	47
4.1	Summary of key vectors and matrices used in MIMO channel shortening scheme.	54
4.2	Achievable bit rate comparison ($\Gamma = 9.8$ dB, $p = 512$, $q = 13$, $\nu = 32$, $N = 512$, $L = 2$, $P = 2$)	55
B.1	Dominant poles and zeros of 8 CSA loops	71

Abstract

Cyclic-prefixed multicarrier communication systems like orthogonal frequency division multiplexing (OFDM) and discrete multitone (DMT) are popular transmission formats for emerging 4G mobile communications and currently standardized in Wireless LAN/MAN and asymmetric digital subscribe line (ADSL) and very-high-bit-rate digital subscriber line (VDSL) modems. In ADSL receiver, a time domain equalizer (TEQ) is generally employed to shorten the long channels to a predefined length to compensate for channel dispersion. Various eigenfilter-based channel shortening methods have been reported in the literature. However, most of them introduce deep nulls in the frequency response, leading to suppression of some potential subcarriers and bit rate fall. Besides, optimum minimization of delay spread of the channel in noise is also not addressed in the literature so far.

The main focus of this work is twofold: the primary goal is to propose and analyze several non-adaptive and adaptive algorithms for the TEQ design. A number of unaddressed issues such as removal of spectral nulls in TEQ frequency response, minimization of delay spread in noise and optimum shortening with reduced transmission delay sensitivity are incorporated in the proposed modifications for optimal bit rate and interference performance. The secondary goal is to extend one of the low complexity single channel TEQ design algorithm to jointly shorten multiple input multiple output (MIMO) channels. Extensive simulations are carried out to compare the performance of the proposed methods with several state-of-the-art techniques.



Chapter 1

Introduction

1.1 Channel shortening

The capacity of reliable information transmission over any physical communication channel is limited by non-ideal characteristics of the channel. Among those impairments encountered in a discrete time channel, intersymbol interference (ISI) due to channel memory corrupts the current received data by previous data symbols. Severe ISI significantly downgrades the achievable bit rate. Some form of channel equalization is typically employed by a digital transmission system to mitigate the ISI.

The goal of equalization for single carrier transmission systems is to design an equalizer such that the convolution of the channel and equalizer is a Kronecker delta, i.e., an impulse at some delay Δ and zero otherwise. In multicarrier transmission systems [7], such as for DMT based ADSL system or OFDM for wireless communications, the problem is more general. The delay spread of the transmission channel must be within a predefined length, and the equalizer is designed such that the convolution of the channel and equalizer produces an effective channel that has been shortened to this length. This design problem is referred to as *channel shortening*.

The goal is to shorten the long channel impulse response to a reasonable length (rather to an impulse) by the aid of a receiver filter (i.e., equalizer) under some criterion and constraints. See Fig. 1.1 for illustration. This thesis concerns channel equalization for DMT based wireline ADSL communication systems. First, an overview of baseband DMT system will be given which will be followed by discussion on channel equalization for multicarrier systems.

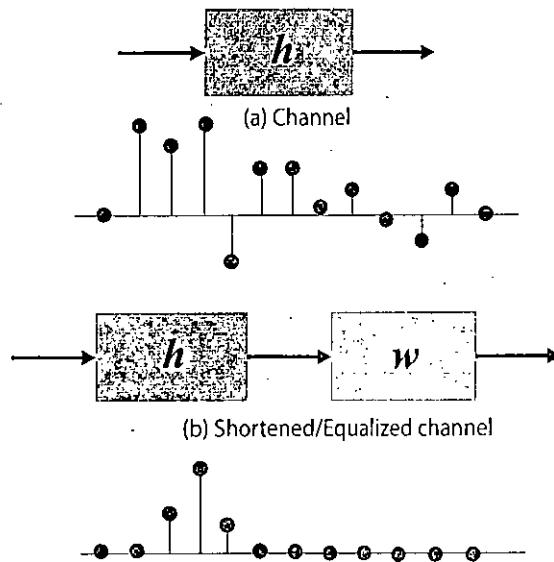


Fig. 1.1: Illustration of channel shortening with a receiver filter. Here, h and w denote channel and equalizer, respectively.

1.2 Discrete multitone modulation

ISI is a major problem associated with broadband channels. This undesirable effect is caused by the spectral shaping of the channel. In other words, variation of magnitude and phase responses of the channel over frequency causes neighboring symbols to interfere with each other at the receiver. Two approaches to combat ISI are full channel equalization and multicarrier modulation (MCM).

Full channel equalization undoes the spectral shaping effect of a channel using a filter which is called an equalizer. Although linear equalizers are easy to implement, they enhance noise and thus degrade the performance of the system. Therefore, more complicated nonlinear equalizers such as the decision feedback equalizer, have been proposed. One of the drawbacks of nonlinear equalizers is their high computational complexity, especially under high sampling rates.

MCM is one possible solution for high-speed digital communications. In contrast to single carrier modulation, MCM,

- avoids full equalization of a channel,
- uses available bandwidth efficiently by controlling the power and number of bits in each subchannel,

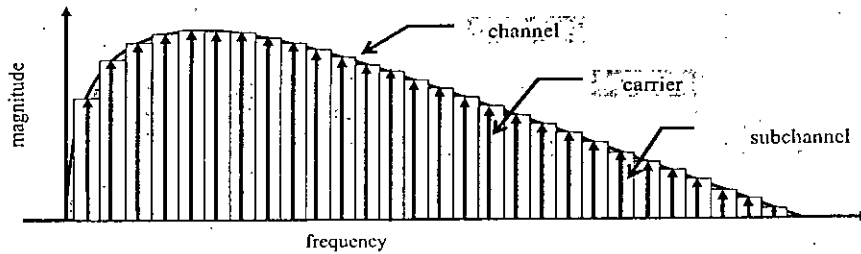


Fig. 1.2: Channel Bandwidth and Multicarrier Modulation. DMT Modulation has subchannels that are 4.3125 kHz wide in ADSL [1].

- is robust against impulsive noise and fast fading due to its long symbol duration, and
- avoids narrowband distortion by simply disabling one or more subchannels.

MCM has been standardized for G.DMT and G.lite ADSL [1] as well as digital audio/video broadcasting [8], [9] and also proposed for 4G mobile communications and VDSL applications.

In multicarrier modulation, the channel is partitioned into a large number of small bandwidth channels called subchannels. If a subchannel is narrow enough so that the channel gain in the subchannel is approximately a complex constant, then no ISI would occur in this subchannel. Thus, information can be transmitted over these narrowband subchannels without ISI, and the total number of bits transmitted is the sum of the number of bits transmitted in each subchannel. If the available power were distributed over the subchannels using the SNR of each subchannel, then high spectral efficiency could be achieved. See Fig. 1.2 for illustration.

Efficiently dividing the channel into hundreds of subchannels became tractable only in the 1990s with the cost vs. performance provided by programmable digital signal processors and the advancement in digital signal processing methods [7]. One of the most efficient ways to partition a channel into large number of narrowband channels is the fast Fourier transform (FFT) [7]. Multicarrier modulation implemented via a FFT is called Discrete Multitone (DMT) modulation or Orthogonal Frequency Division Multiplexing (OFDM). DMT is more common in wireline applications, whereas OFDM is more common for wireless applications. In transmission, the key difference between the two methods is in the assignment of bits to each subchannel.

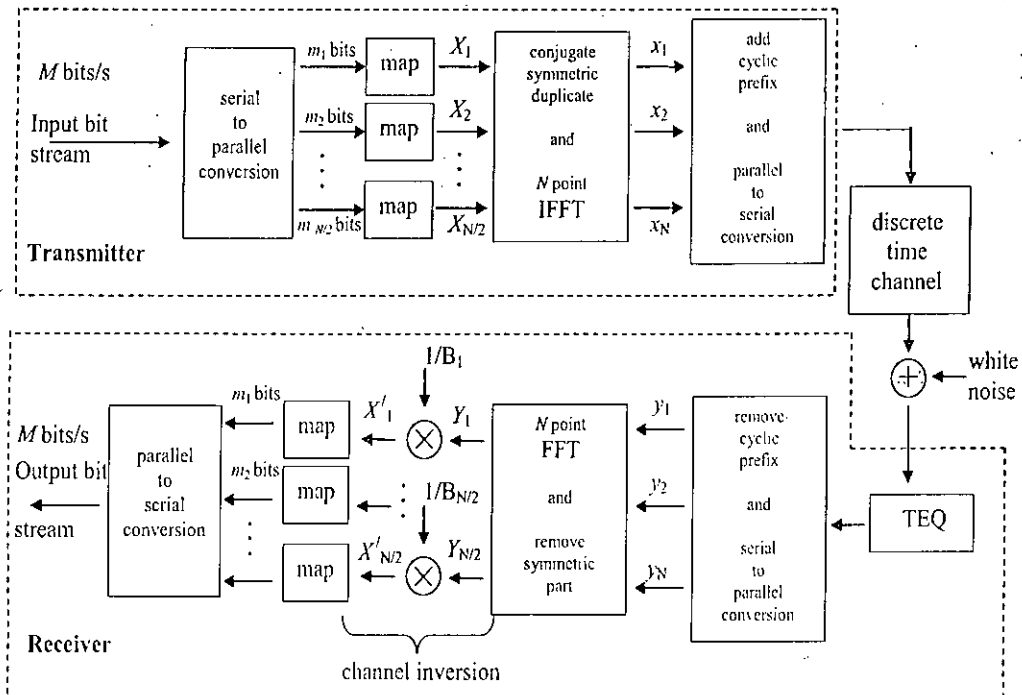


Fig. 1.3: Block diagram of a multicarrier modulation system. N denotes (1)FFT size, B denotes channel frequency coefficients.

1.2.1 DMT transmitter

A block diagram of a DMT (or OFDM) transceiver is shown in Fig. 1.3. In the transmitter, M bits of the input bit stream are buffered. These bits are then assigned to each of the $N/2$ subchannels using a bit loading algorithm [7]. In DMT systems, bit loading algorithms assign the bits and available power to each subchannel according to the SNR in each subchannel, such that high SNR subchannels receive more bits than low SNR subchannels. Extremely low SNR subchannels are not used. In OFDM systems, usually the number of bits in each channel is equal and constant. Thus, there is no need for a bit loading algorithm.

The second step is the mapping of the assigned bits to subsymbols using a modulation method, such as QAM in ADSL modems. These subsymbols are complex-valued in general and can be thought of being in the frequency domain. The efficiency of DMT and OFDM lies in the modulation of the subcarriers. Instead of having $N/2$ independent modulators, the modulators are implemented with an N -point inverse FFT (IFFT). In order to obtain real samples after IFFT,

the $N/2$ subsymbols are duplicated with their conjugate symmetric counterparts. The obtained time domain samples are called a DMT symbol.

A guard period between DMT symbols is used to prevent ISI. It is implemented by prepending a symbol with its last ν samples, which is called a cyclic prefix (CP). Thus, one block consists of $N + \nu$ samples instead of N samples, which reduces the channel throughput by a factor of $(N + \nu)/N$. ISI is completely eliminated for channels with impulse responses of length less than or equal to $\nu + 1$. The prefix is selected as the last ν samples of the symbol in order to convert the linear convolution effect of the channel into circular convolution and help the receiver perform symbol synchronization. Circular convolution can be implemented in the DFT domain by using the FFT. After the FFT in the receiver, the subsymbols are the product of the N -point FFT of the channel impulse response and the N -point FFT of the transmitted subsymbols.

1.2.2 DMT receiver

The receiver is basically the dual of the transmitter with the exception of the addition of time-domain and frequency domain equalizers. The time-domain equalizer (TEQ)¹ ensures that the equalized channel impulse response is shortened to be less than the length of the CP. If the TEQ is successful, then the received complex subsymbols after the FFT are the multiplication of the transmitted subsymbols with the FFT of the shortened (equalized) channel impulse response. The frequency domain equalizer (also called a one-tap equalizer) divides the received subsymbols by the FFT coefficients of the shortened channel impulse response. After mapping the subsymbols back to the corresponding bits using the QAM constellation, they are converted to serial bits.

1.3 Equalization for discrete multitone modulation

With DMT, the problem of fully equalizing a channel is converted into partitioning the channel into small subchannels which is more efficient to implement in high-speed transmission. As the subchannels are orthogonal to each other, this type of modulation is inherently resistant to Inter-Carrier Interference (ICI). Fig.

¹TEQs are also known as channel shortening equalizers

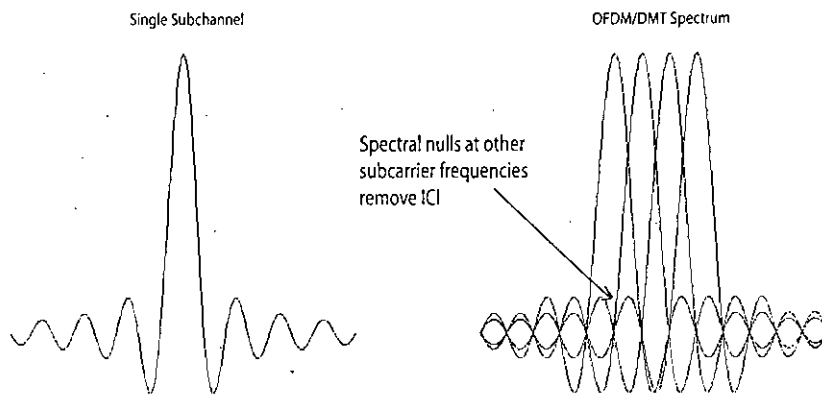


Fig. 1.4: Illustration of OFDM spectrum. In each sample of FFT grid, one subcarrier has peak while others have nulls.

1.4 shows a typical OFDM spectrum. However, this does not imply that equalization is not required in an DMT system. The spectra of each inverse FFT (IFFT) modulated subchannel is a sampled sinc function which is not bandlimited. Demodulation is still possible due to the orthogonality between the *sinc* functions. An ISI causing channel, however, destroys orthogonality between subchannels so that they cannot be separated at the receiver.

One way to prevent ISI is to use a guard period between two successive DMT symbols (one DMT symbol consists of N samples where $N/2 + 1$ is the number of subchannels). This guard period has to be at least as long as the channel impulse response. Since no new information is transmitted in this guard period, the channel throughput reduces proportionally to the length of it. If the channel impulse response is relatively long compared to the symbol length, then this performance loss can be prohibitive.

One way to reduce ISI with a shorter cyclic prefix is to use an equalizer. Since the length of a DMT symbol is longer than a symbol in single carrier modulation, equalization is simpler. This accordingly allows us to use a shorter-length cyclic prefix and minimize reduction in throughput.

The ADSL standard uses a guard period, time-domain equalization, and frequency-domain equalization. The TEQ shortens the channel to a length of a predetermined but short guard period.

The problem of TEQ design in the DMT transceivers may be formulated as follows. Given a channel with the impulse response samples $h(0), h(1), \dots, h(L_h -$

1), where $L_h - 1 =$ FIR channel order, and might be corrupted with some additive noise, we wish to find the coefficients $w(0), w(1), \dots, w(L_w - 1)$, where $L_w - 1 =$ filter order, of a transversal equalizer that results in a combined channel-equalizer response which is shortened to a duration of L_s samples, where L_s can be at most equal to the length of cyclic prefix (CP) ν plus one. In this thesis, the known parameters are the channel response, the channel noise (usually its autocorrelation coefficients), and the expected duration L_s of the equalized response. The criterion used for the selection of the equalizer may vary such as shortening SNR (SSNR), signal to interference plus noise ratio, delay spread, output SNR etc. However, the ultimate goal in the design of the TEQ is to achieve maximum bit rate over the channel, given an acceptable level of bit-error probability. But, development of a practical design method that can achieve this goal turns out to be very difficult. Most of the studies focus bit rate maximizing in a sub-optimal way. Thus there is a scope for development of improved TEQ design methods that can provide optimum performance.

1.4 Objective of the thesis

This thesis focuses on optimum time domain equalizer design with respect to different performance metrics. The objectives of this work are described below:

1. Design of noise optimized minimum delay spread equalizer for DMT transceivers. The proposed iterative TEQ design method will attempt to jointly minimize delay spread of the channel and filtered noise at the output of the equalizer.
2. Development of an improved eigenfilter method for TEQ design for DMT systems. The proposed cost function, along with good channel shortening, will avoid spectral nulls in the useful signal band seen in most of the reported eigenfilter based methods. To reduce computational complexity of the proposed algorithm, a heuristic technique to determine the optimum transmission delay is also proposed.
3. Development of an iterative MSSNR design method which does not need Cholesky factor computation, less sensitive to transmission delay and suitable for arbitrary length TEQ. Step size adaptation will also be incorporated

to improve convergence performance. Since the iterative design would approximate MSSNR design, it is expected that severe nulls would be less prominent in the useful signal band. The iterative technique can also be readily applicable to other eigenfilter based technique as well.

4. Development MIMO TEQ design algorithm for cyclic-prefixed block transmission systems based on maximizing SSNR. Goal of the proposed channel shortening method is to jointly shorten MIMO ISI channels. The MIMO TEQ is formed with eigenvectors corresponding to some maximum eigenvalues of a particular matrix. The method will be suitable for any arbitrary length TEQ as well. Composite bit rate formula is also proposed to compare achievable channel capacity performance.

1.5 Organization of this thesis

This thesis consists of five chapters. Chapter 1 discusses the basics of channel shortening, its importance in multicarrier communication systems, general problem statement and the objectives of this work.

In Chapter 2, a brief review of the state-of-the-art eigenfilter based TEQ design methods are discussed. At first, the methods are presented under common mathematical framework and then the shortcomings of the reported methods are analyzed with different crucial results.

In Chapter 3, several TEQ design algorithms are proposed which address the shortcomings of the reported methods. First, noise optimized minimum delay spread equalizer design method is presented. The minimum delay spread design problem is formulated, then true time reference is derived with respect to which delay spread will be minimized. Besides, cost function to minimize noise at the output of the equalizer is also modeled. Then, iterative TEQ design method is presented. Second, an improved low complexity eigenfilter based TEQ design method is proposed. Heuristic technique to compute optimum delay Δ is then formulated. Third, iterative MSSNR method is developed. Initially, modified cost function for MSSNR design is presented to develop cost function for iterative algorithm and then expression for adaptive step size is derived. Simulation results follow the analysis of each of the designs to corroborate the claim on performance

improvement.

In Chapter 4, MIMO channel shortening algorithm is proposed. First, MIMO system model is presented which is followed by formulation of MIMO channel shortening problem based on maximizing shortening SNR. Then, optimum MIMO TEQ design algorithm is derived. Simulation results for the algorithm are then provided which include performance comparison on the basis of common figure of metrics.

Finally conclusions and suggestions for future works are provided in Chapter 5.

Chapter 2

Eigenfilter based TEQ design methods: Literature survey

2.1 Introduction

“When we mean to build, we first survey the plot, then draw the model.”

- William Shakespeare, *Henry IV Part II*, Act I, Scene iii.

Prior to presenting the methods developed in this thesis for TEQ design, this chapter briefly reviews previous work on the matter. Various equalizer design methods are discussed in the literature in the context of multicarrier transceivers that are related to the proposed designs discussed in this thesis. The chapter provides a unified mathematical framework for the eigenfilter based equalizer design.

2.2 Common TEQ design formulation

There are many ways of designing the equalizer for DMT systems depending on disparate optimization criteria. However, almost all of the algorithms fit into the same formulation: the maximization of a generalized Rayleigh quotient [10] or a product of generalized Rayleigh quotients [11], [12]. Consider, the following optimization problem

$$\mathbf{w}_{opt} = \arg \max_{\mathbf{w}} \prod_{j=1}^M \frac{\mathbf{w}^T \mathbf{X}_j \mathbf{w}}{\mathbf{w}^T \mathbf{Y}_j \mathbf{w}} \quad (2.1)$$

In general, the solution to (2.1) is not well-understood when $M > 1$. However, for $M = 1$,

$$\mathbf{w}_{opt} = \arg \max_{\mathbf{w}} \frac{\mathbf{w}^T \mathbf{X} \mathbf{w}}{\mathbf{w}^T \mathbf{Y} \mathbf{w}} \quad (2.2)$$

the solution is the generalized eigenvector of the matrix pair (\mathbf{X}, \mathbf{Y}) corresponding to the largest generalized eigenvalue [13]. Equivalently, the inverse of the ratio in (2.2) is minimized by the eigenvector of (\mathbf{X}, \mathbf{Y}) corresponding to the smallest generalized eigenvalue. Most TEQ designs fall into the category of (2.2). The vector \mathbf{w} to be optimized is usually the TEQ, but it may also be e.g. the (shortened) target impulse response (TIR) [14], the per-tone equalizer [15], or half of a symmetric TEQ [16].

TEQ designs of the form of (2.2) include the Minimum Mean Squared Error (MMSE) design [14], [3], the Maximum Shortening SNR (MSSNR) design [4], [17], the MSSNR design with a unit norm TEQ constraint (MSSNR-UNT) or a symmetric TEQ constraint (Sym-MSSNR) [18], the Minimum Inter Symbol Interference (Min- ISI) design [19], the Minimum Delay Spread (MDS) design [5] etc.

The generalized eigenvector problem requires computation of the \mathbf{w} that satisfies [13]

$$\mathbf{X} \mathbf{w} = \lambda \mathbf{Y} \mathbf{w} \quad (2.3)$$

where \mathbf{w} is the eigenvector corresponding to the largest generalized eigenvalue λ . When \mathbf{Y} is invertible, real and symmetric, one approach to solve (2.3) is to form the Cholesky decomposition $\mathbf{Y} = \sqrt{\mathbf{Y}} \sqrt{\mathbf{Y}}^T$, and define $\mathbf{v} = \sqrt{\mathbf{Y}} \mathbf{w}$, then

$$\mathbf{v}_{opt} = \arg \max_{\mathbf{v}} \frac{\mathbf{v}^T \overbrace{(\sqrt{\mathbf{Y}}^{-1} \mathbf{X} \sqrt{\mathbf{Y}}^T)}^{\mathbf{Z}} \mathbf{v}}{\mathbf{v}^T \mathbf{v}} \quad (2.4)$$

The solution for \mathbf{v} is the eigenvector of \mathbf{Z} associated with the largest eigenvalue, and $\mathbf{w}_{opt} = \sqrt{\mathbf{Y}}^{-T} \mathbf{v}_{opt}$, assuming that \mathbf{Y} is invertible. If \mathbf{Y} is not invertible, then it has a non-zero null space, so the ratio is maximized (to infinity!) by choosing \mathbf{w} to be a vector in the null space of \mathbf{Y} . In some cases, \mathbf{Y} or \mathbf{X} is the identity matrix, in which case (2.3) reduces to a traditional eigenvalue problem. Examples include the computation of the MMSE target impulse response (TIR) [14], the MSSNR

TEQ with a unit norm constraint on the TEQ [18], the MDS algorithm [5]. There are a variety of all-purpose methods available for finding extreme eigenvectors, such as the power method [10] and conjugate gradient methods [20] etc. than can be used to solve (2.3).

2.3 Single Rayleigh quotient cases

Several common TEQ designs that are designed by maximizing a generalized Rayleigh quotient are the the maximum shortening SNR (MSSNR) design [4], [17], minimum mean squared error (MMSE) design [3], [14], the minimum inter-symbol interference (Min-ISI) design [19], the minimum delay spread (MDS) design [5] etc. and their variants. This section provides a brief description of these design methods.

2.3.1 The Maximum Shortening SNR (MSSNR) method

The MSSNR TEQ design proposed by Melsa, Younce and Rohrs in [4] attempts to maximize the ratio of the energy in a window of the effective channel over the energy in the remainder of the effective channel. The MSSNR design was reformulated for numerical stability by Yin and Yue in [17]. Following [4], let

$$\mathbf{H}_{des} = \begin{bmatrix} h(\Delta) & h(\Delta - 1) & \dots & h(\Delta - L_w + 1) \\ \vdots & & \ddots & \vdots \\ h(\Delta + \nu) & h(\Delta + \nu - 1) & \dots & h(\Delta + \nu - L_w + 1) \end{bmatrix} \quad (2.5)$$

as the middle $\nu + 1$ rows of the (tall) channel convolution matrix \mathbf{H} , and \mathbf{H}_{res} as the remaining rows of \mathbf{H} :

$$\mathbf{H}_{res} = \begin{bmatrix} h(0) & 0 & \dots & 0 \\ \vdots & & \ddots & \vdots \\ h(\Delta - 1) & h(\Delta - 2) & \dots & h(\Delta - L_w) \\ h(\Delta + \nu + 1) & h(\Delta + \nu) & \dots & h(\Delta + \nu - L_w + 2) \\ \vdots & & \ddots & \vdots \\ 0 & 0 & \dots & h(L_h - 1) \end{bmatrix} \quad (2.6)$$

Thus, $\mathbf{c}_{des} = \mathbf{H}_{des}\mathbf{w}$ yields a length $\nu + 1$ window of the effective channel (see Fig. (2.1)), and $\mathbf{c}_{res} = \mathbf{H}_{res}\mathbf{w}$ yields the remainder of the effective channel. The MSSNR design problem can be stated as “maximize $\|\mathbf{c}_{des}\|$ subject to the

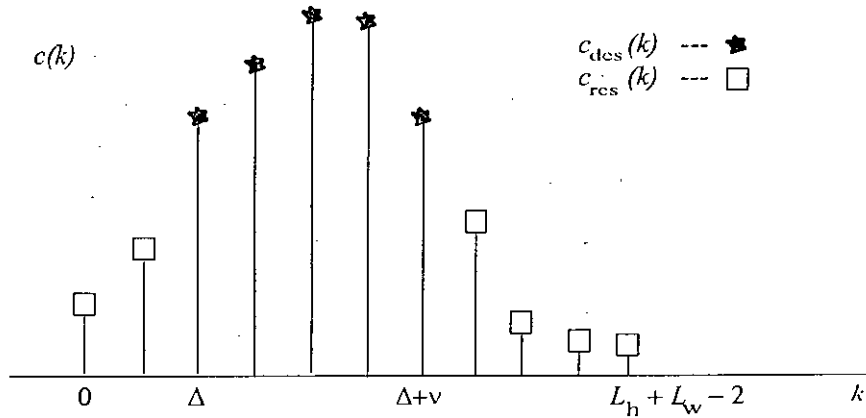


Fig. 2.1: Decomposition of the effective channel $c(k)$ into a desired channel $c_{des}(k)$ and residual channel $c_{res}(k)$. Δ denotes transmission delay.

constraint $\| \mathbf{c}_{res} \| = 1$, [4], [17] which reduces to (2.2) with

$$\mathbf{Y} = \mathbf{H}_{res}^T \mathbf{H}_{res} \quad (2.7)$$

$$\mathbf{X} = \mathbf{H}_{des}^T \mathbf{H}_{des} \quad (2.8)$$

It may be stated another way as: optimize \mathbf{w} to maximize $\mathbf{w}^T \mathbf{X} \mathbf{w}$ subject to $\mathbf{w}^T \mathbf{Y} \mathbf{w} = 1$. Or equivalently, optimize \mathbf{w} to minimize $\mathbf{w}^T \mathbf{Y} \mathbf{w}$ subject to $\mathbf{w}^T \mathbf{X} \mathbf{w} = 1$ [17].

2.3.2 The Minimum Mean Squared Error (MMSE) method

The MMSE design [14], originally intended for complexity reduction in maximum likelihood sequence estimation (MLSE), is similar to the MSSNR design, although it takes noise into account. Indeed, for a white input and no noise, the MMSE and MSSNR designs are identical [21]. The system model for the MMSE solution is shown in Fig (2.2). It creates a virtual target impulse response (TIR) \mathbf{b} of length $\nu + 1$ such that the MSE, which is measured between the output of the effective channel and the output of the TIR, is minimized.

The MMSE TEQ and TIR must satisfy [3], [14]

$$\mathbf{R}_{rx} \mathbf{b} = \mathbf{R}_r \mathbf{w} \quad (2.9)$$

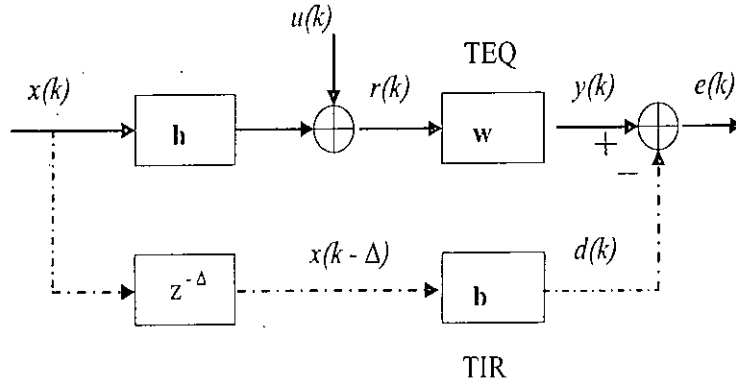


Fig. 2.2: MMSE system model. The symbols \mathbf{h} , \mathbf{w} , and \mathbf{b} are the impulse responses of the channel, the TEQ, and the target, respectively. Here, Δ represents transmission delay. The dashed lines indicate a virtual path, which is used only for analysis.

where

$$\mathbf{R}_{rx} = E \left[\begin{bmatrix} r(k) \\ \vdots \\ r(k - L_w) \end{bmatrix} \begin{bmatrix} x(k - \Delta) & \cdots & x(k - \Delta - \nu) \end{bmatrix} \right] \quad (2.10)$$

is the channel input-output cross-correlation matrix and

$$\mathbf{R}_r = E \left[\begin{bmatrix} r(k) \\ \vdots \\ r(k - L_w) \end{bmatrix} \begin{bmatrix} r(k) & \cdots & r(k - L_w) \end{bmatrix} \right] \quad (2.11)$$

is the channel output autocorrelation matrix. Typically, \mathbf{b} is computed first, and then (2.9) is used to determine \mathbf{w} . The goal is that $\mathbf{h} * \mathbf{w}$, the convolution of \mathbf{h} and \mathbf{w} , approximates a delayed version of \mathbf{b} . The TIR is the eigenvector corresponding to the minimum eigenvalue of [14]

$$\mathbf{R}_\Delta = \mathbf{R}_x - \mathbf{R}_{xr} \mathbf{R}_r^{-1} \mathbf{R}_{rx} \quad (2.12)$$

where $\mathbf{R}_{xr} = \mathbf{R}_{rx}^T$ and

$$\mathbf{R}_x = E \left[\begin{bmatrix} x(k) \\ \vdots \\ x(k - \nu) \end{bmatrix} \begin{bmatrix} x(k) & \cdots & x(k - \nu) \end{bmatrix} \right] \quad (2.13)$$

is the input autocorrelation matrix. It is because the mean square error $J = E[e^2(k)]$ will yield a quadratic form in \mathbf{b} as

$$J = \mathbf{b}^T \mathbf{R}_\Delta \mathbf{b} \quad (2.14)$$

Hence, the problem reduces to (2.2) with

$$\mathbf{Y} = \mathbf{R}_\Delta \quad (2.15)$$

$$\mathbf{X} = \mathbf{I}_{\nu+1} \quad (2.16)$$

In this criteria, a unit energy constraint (UEC) $\mathbf{b}^T \mathbf{b} = 1$ is applied to the TIR coefficients to avoid the trivial null TEQ solution.

2.3.3 The Minimum Inter-Symbol Interference (Min-ISI) method

The MSSNR design has spawned many extensions and variations. The Min-ISI method shapes the residual energy in the tails of the channel in the frequency domain, with the goal of placing the excess energy in unused frequency bins [19]. The idea is to penalize the residual interference according to which subchannel it is in. Subchannels with higher signal power have higher weights, hence the residual interference is penalized more. The \mathbf{Y} and \mathbf{X} matrices are more complicated in this case. The design is a minimization of a generalized Rayleigh quotient with [19]

$$\begin{aligned} \mathbf{Y} &= \widehat{\mathbf{H}}_{res}^T \sum_{i \in S_u} (\mathbf{q}_i \frac{S_{x,i}}{S_{n,i}} \mathbf{q}_i^H) \widehat{\mathbf{H}}_{res} \\ \mathbf{X} &= \widehat{\mathbf{H}}_{des}^T \widehat{\mathbf{H}}_{des} \end{aligned} \quad (2.17)$$

where $\widehat{\mathbf{H}}_{res}$ is equal to \mathbf{H}_{res} padded with zeros in the middle, $S_{x,i}$ is the transmitted signal power in tone i , $S_{n,i}$ is the received noise power in tone i , S_u is the set of used tones, and \mathbf{q}_i is the i th coefficient DFT vector. If all the tones were used and if $S_{x,i}/S_{n,i}$ were constant across all the tones, then the Min-ISI matrices in (2.17) would reduce to the MSSNR matrices in (2.7). Thus, the MSSNR design is a special case of the Min-ISI design.

2.3.4 The Minimum Delay Spread (MDS) method

The taps of \mathbf{h} exceeding the CP length cause ISI and ICI, and the interference levels depend on both the taps' distances to the prefix and their energy [5]. The contributions of interblock interference (IBI) from tails of impulse responses grow linearly as the samples move away to the edges [22]. This fact is partially ignored by MSSNR approach since a rectangular window is used without bias on the

distance issue. Therefore, Schur and Speidel in [5] proposed to use an exponential window instead to minimize the square of the delay spread of effective channel \mathbf{c} , where the delay spread is defined as

$$D = \sqrt{\frac{1}{E} \sum_{k=0}^{L_c-1} (k - \eta)^2 |c(k)|^2} \quad (2.18)$$

Here, $E = \mathbf{c}^T \mathbf{c}$, and η is a user-defined center of mass or centroid. This results in (2.2) with

$$\mathbf{Y} = \mathbf{H}^T \mathbf{Q} \mathbf{H} \quad (2.19)$$

$$\mathbf{X} = \mathbf{H}^T \mathbf{H} \quad (2.20)$$

where \mathbf{Q} is a diagonal weighting matrix defined as

$$\mathbf{Q} \triangleq \text{diag}([(0 - \eta)^2, (1 - \eta)^2, \dots, (L_c - 1 - \eta)^2]) \quad (2.21)$$

2.4 Shortcomings of reported eigenfilter methods

2.4.1 MSSNR method

Though MSSNR method performs relatively well with relatively low complexity, on account of the fact that the design problem is an eigenfilter-type problem, it suffers from several shortcomings. First, the method does not account for any effects due to noise present in the system. Furthermore, the Cholesky decomposition depends on the delay parameter Δ for the formulation in (2.7). If we wish to vary Δ over a certain region to see which value performs the best, which is typically done in practice, then a new Cholesky factor must be computed for each Δ . This results in an extra computational load for each Δ considered.

Since $\mathbf{H}^T \mathbf{H} = \mathbf{H}_{res}^T \mathbf{H}_{res} + \mathbf{H}_{res}^T \mathbf{H}_{res}$, it is mathematically equivalent to minimize the residual energy over the total channel energy [2] (See appendix A), with

$$\mathbf{Y} = \mathbf{H}_{res}^T \mathbf{H}_{res} \quad (2.22)$$

$$\mathbf{X} = \mathbf{H}^T \mathbf{H} \quad (2.23)$$

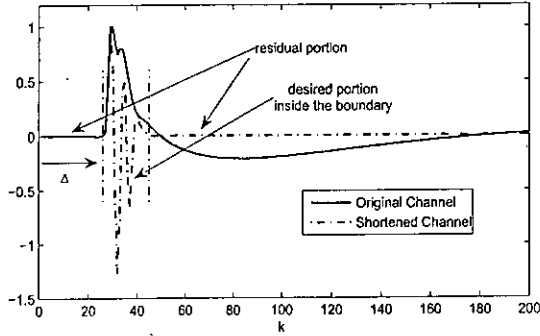


Fig. 2.3: Original and shortened channel by MSSNR method. TEQ length = 17, Channel length = 512, window length $\nu + 1 = 32$. Only first 200 samples are shown.

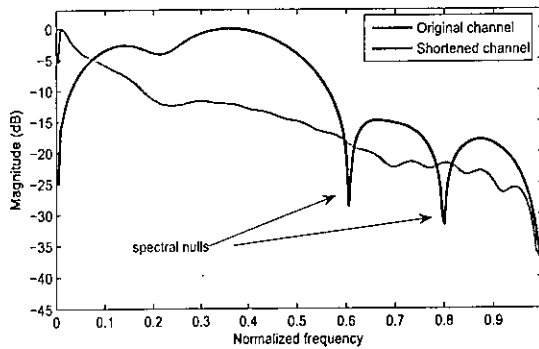


Fig. 2.4: Magnitude response of original and shortened channel by MSSNR method.

or to maximize the energy inside the window over the total channel energy [23], with

$$\mathbf{Y} = \mathbf{H}^T \mathbf{H} \quad (2.24)$$

$$\mathbf{X} = \mathbf{H}_{des}^T \mathbf{H}_{des} \quad (2.25)$$

This technique results in a reduced-complexity implementation because in (2.22), Cholesky factor computation for matrix \mathbf{X} is to be determined only once as \mathbf{X} does not depend on delay. Typical plot of shortened channel by MSSNR method is shown in Fig. 2.3.

The MSSNR method, however, uses only the channel impulse response when calculating the optimum TEQ, which means that it ignores the effect of noise and transmit power spectrum. Since, the bit rate is a function of noise, channel gain, and transmit power spectrum, a bit rate optimal method must take into account

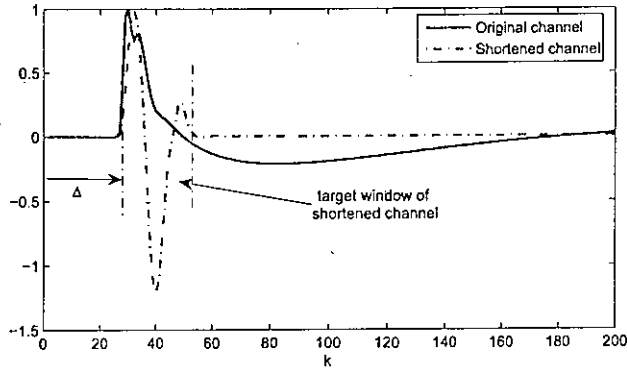


Fig. 2.5: Original and shortened channel by MMSE method. TEQ length = 17, Channel length = 512, window length $\nu + 1 = 32$. Only first 200 samples are shown.

all three when computing the optimum TEQ. As a consequence, the MSSNR method cannot optimize bit rate.

Furthermore, TEQs designed by MSSNR method tend to insert zeros close to unit circle which causes spectral nulls to form at those frequencies. This act sometimes kills potential subcarriers to carry data bits and thereby reduce bit rate. Frequency response of shortened channel by MSSNR method is shown in Fig. 2.4.

Despite these shortcomings, the low complexity MSSNR method in [4] represented the first attempt to pose the channel shortening problem as an eigenfilter-type problem.

2.4.2 MMSE method

MMSE method takes channel noise into consideration which MSSNR method does not [3], [14]. However, once \mathbf{b} has been appropriately computed, the equalizer coefficients of \mathbf{w} must still need to be found using the orthogonality principle (See (2.9)). Again, minimizing MSE does not necessarily minimize the residual portion outside the target window. Shortened channel by MMSE methods is shown in Fig. 2.5.

It is also possible to solve for the TEQ directly, without first computing the TIR. For a white input signal, the MMSE TEQ can be designed directly using

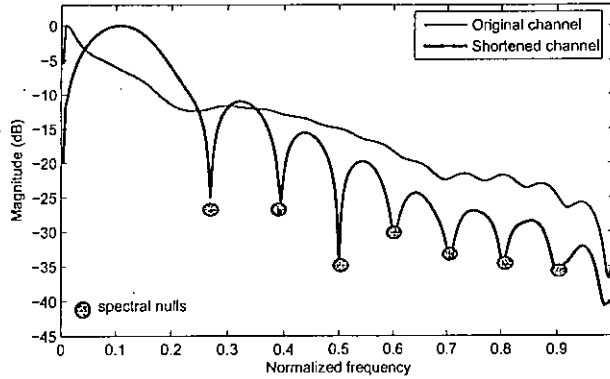


Fig. 2.6: Magnitude response of original and shortened channel by MMSE method.

(2.2) with [16]

$$\mathbf{Y} = \mathbf{H}_{res}^T \mathbf{H}_{res} + \mathbf{R}_n \quad (2.26)$$

$$\mathbf{X} = \mathbf{H}_{des}^T \mathbf{H}_{des} \quad (2.27)$$

where \mathbf{R}_n is the noise autocorrelation matrix of size $L_w \times L_w$.

The aforementioned MMSE methods do not have control over the frequency response of the TEQ. For example, a TEQ designed with these methods would have some gain over unused subchannels which would contribute only to the noise and not to the desired signal. Also, many MMSE optimal TEQs have deep nulls in the frequency domain. Those subchannels with deep nulls become useless. See Fig. 2.6.

2.4.3 Min-ISI method

Min-ISI method is in fact a variant of MSSNR method. This method places residual portion in subchannels with high noise power. However, as with the MSSNR method of [4], the Cholesky factor needed in (2.17) [19] depends on the delay parameter Δ which entails solving generalized EV problem for each delay. Shortened channel by Min-ISI method is shown in Fig. 2.7. Furthermore, Min-ISI method is relatively more complex than MMSE and MSSNR methods (which is clear from definitions of \mathbf{X} and \mathbf{Y} in (2.17)) [11].

This method, as it accounted for both ISI and noise, was shown to perform nearly optimally in terms of bit rate. However, this method also exhibits spectral

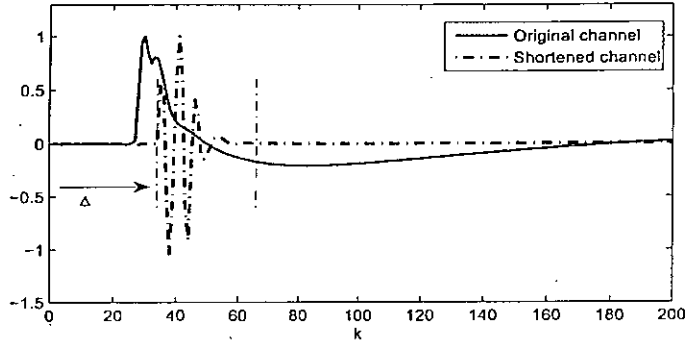


Fig. 2.7: Original and shortened channel by Min-ISI method. TEQ length = 17, Channel length = 512, window length $\nu + 1 = 32$. Only first 200 samples are shown.

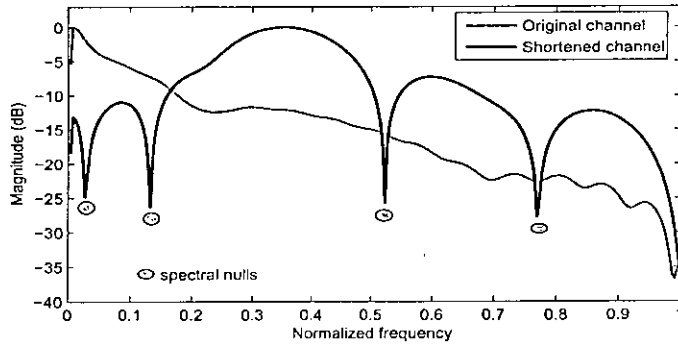


Fig. 2.8: Magnitude response of original and shortened channel by Min-ISI method.

nulls in certain useful subchannels like MSSNR and MMSE methods. See Fig. 2.8.

2.4.4 MDS method

Unlike MSSNR, MMSE and Min-ISI methods, the Cholesky factor required for the MDS method [5] does not depend on the delay parameter Δ . Hence, the method is very low in complexity as only one Cholesky factor must be computed for all Δ (See, \mathbf{X} in (2.21) does not depend on delay). Despite this significant decrease in complexity, the method suffers from several shortcomings. Though the method was shown to be less prone to synchronization errors than others, it does not account for the desired channel length $\nu + 1$ or any knowledge of the noise statistics. From Fig. 2.9, it is clear that shortened channel spans more than the target window length of $\nu + 1$ hence causes severe ISI.

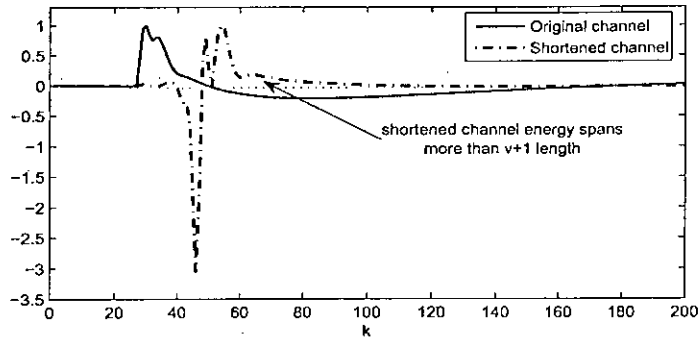


Fig. 2.9: Original and shortened channel by MDS method. TEQ length = 17, Channel length = 512. Only first 200 samples are shown.

2.5 Conclusion

In this chapter, some state-of-the-art eigenfilter based channel shortening equalizers are described and their shortcomings are presented. The loss in performance shown by the reported methods acts as motivation for the work presented in the later chapters.

Chapter 3

Development of optimum channel shortening algorithms

3.1 Introduction

In the previous chapter, several shortcomings of state-of-the-art eigenfilter methods are addressed such as undesired spectral attenuation, delay sensitivity and need for Cholesky factor computation for each delay. In this chapter, three channel shortening algorithms are proposed to address these issues. First, the computationally efficient MDS method is modified to account for the noise and true time reference. Second, the MDS method is further improved by incorporating the knowledge of cyclic prefix and adjustment for spectral attenuation. Besides, an iterative MSSNR design method is proposed that not only removes the drawbacks of the direct MSSNR method but also achieves performance very close to the direct solution. Extensive simulations are carried out to analyze the performance of the proposed methods.

3.2 System model

The channel/equalizer model is shown in Fig. 3.1 and the notation summarized in Table 3.1. We make the following assumptions here.

- The channel, $\mathbf{h} \triangleq [h(0), h(1), \dots, h(L_h - 1)]^T$ is known to be finite impulse response (FIR) filter of length L_h .
- The TEQ, $\mathbf{w} \triangleq [w(0), w(1), \dots, w(L_w - 1)]^T$ is known to be FIR filter of length L_w .

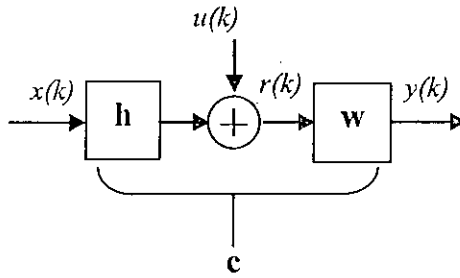


Fig. 3.1: System model with channel/equalizer.

Table 3.1: Channel shortening notation

Notation	Meaning
ν	length of CP
N	FFT size
Δ	delay of effective channel
\mathbf{h}	$L_h \times 1$ CIR vector
\mathbf{w}	$L_w \times 1$ TEQ impulse response vector
\mathbf{c}	$L_c \times 1$ EIR vector
\mathbf{H}	$L_c \times L_w$ channel convolution matrix
\mathbf{R}_u	$L_w \times L_w$ noise covariance matrix
\mathbf{I}_n	$n \times n$ identity matrix
\mathbf{A}^T	transpose
$\mathbf{1}$	vector of all 1's
$\mathbf{0}$	vector of all 0's
$\text{diag}[]$	diagonal matrix with entries in the main diagonal

- The input $x(k)$ is zero mean and white with variance σ_x^2 .
- The noise $u(k)$ is zero mean wide-sense stationary (WSS) random process with covariance matrix \mathbf{R}_u .
- The processes $x(k)$ and $u(k)$ are uncorrelated.
- The channel, \mathbf{h} is known at the receiver. In practice, channel state information is obtained via training sequence.

The effective channel is given by $c(k) = h(k) * w(k)$ where $*$ denotes linear convolution. Then the output $y(k)$ can be written as

$$\begin{aligned}
 y(k) &= r(k) * w(k) \\
 &= x(k) * h(k) * w(k) + u(k) * w(k) \\
 &= x(k) * c(k) + q(k)
 \end{aligned} \tag{3.1}$$

where $q(k)$ is the filtered noise. In vector form, the effective channel impulse response, \mathbf{c} can be written as

$$\mathbf{c} = \mathbf{H}\mathbf{w} \tag{3.2}$$

where \mathbf{H} is the Toeplitz convolution matrix of the unequalized channel, \mathbf{h} . The effective channel vector is $\mathbf{c} = [c(0), c(1), \dots, c(L_c - 1)]^T$ where $L_c = L_h + L_w - 1$ is the length of effective channel. \mathbf{H} is configured as

$$\mathbf{H} = \begin{bmatrix} h(0) & 0 & \dots & 0 \\ h(1) & h(0) & \dots & \vdots \\ \vdots & \vdots & \ddots & \vdots \\ h(L_h - 1) & h(L_h - 2) & \dots & h(L_h - L_w) \\ 0 & h(L_h - 1) & \dots & h(L_h - L_w + 1) \\ \vdots & \vdots & \ddots & \vdots \\ 0 & 0 & \dots & h(L_h - 1) \end{bmatrix} \tag{3.3}$$

3.3 Noise optimized minimum delay spread TEQ design method

In [5], a unique TEQ design method is proposed which claims to minimize the delay spread of the overall channel impulse response (called MDS method). MDS method is computationally less intensive as it does not require to search for optimum Δ . This approach is independent of the CP length and attempts to squeeze the effective impulse response (EIR) as much as possible. This is advantageous since EIR squeezing allows further to reduce CP length to increase data rate and provides additional robustness to synchronization offset. Recently, in [6], the MDS method is modified to account for the true time reference about which delay spread needs to be minimized. Unfortunately, both of these methods, [5] and [6],

do not take the noise into consideration. Due to noise source models for DMT systems, such as near-end crosstalk (NEXT) and far-end crosstalk (FEXT) [24], it is only natural to exploit such knowledge to obtain a more robust equalizer.

In this section, we generalize the MDS method of to some aspects. First, the cost function is modified to incorporate minimization of noise. Secondly, a trade-off parameter is introduced to set appropriate weights for minimizing delay spread and noise. Thirdly, an iterative algorithm for TEQ update is proposed where the trade-off parameter is adaptively adjusted at each iteration under a specific criterion. Simulation results provided show that our method performs comparatively well in terms of delay spread minimization and filtered noise suppression.

3.3.1 Problem formulation

We restate the definition of the following fundamental quantities from [6] for a given impulse response $\{g(k), -\infty \leq k \leq \infty\}$:

$$E_g = \sum_k g^2(k) \quad (\text{energy}) \quad (3.4)$$

$$k_g = \frac{1}{E_g} \sum_k k g^2(k) \quad (\text{centroid}) \quad (3.5)$$

$$D_g = \sqrt{\frac{1}{E_g} \sum_k (k - k_g)^2 g^2(k)} \quad (\text{delay spread}) \quad (3.6)$$

The MDS design of [5] chooses \mathbf{w} in order to minimize the following cost function:

$$J_{ds} = \frac{1}{E_c} \sum_k (k - k_{ref})^2 c^2(k) \quad (3.7)$$

where E_c is the energy of the effective channel. J_{ds} is, in fact, the square of the delay spread. Hence, [5] actually attempts to minimize the delay spread of the effective channel. This method assumes centroid of the original channel, k_h , as the time reference, k_{ref} . Now, we show that choice of [5] for k_{ref} is not optimum. From (3.7), after some modification, one gets

$$J_{ds} = \frac{1}{E_c} \left\{ \sum_k k^2 c^2(k) - 2k_{ref} \sum_k k c^2(k) + k_{ref}^2 \sum_k c^2(k) \right\} \quad (3.8)$$

Using (3),(4) and setting $\partial J_{ds} / \partial k_{ref}$ equal to zero, we obtain

$$k_{ref} = k_c \quad (3.9)$$

where k_c is the centroid of EIR. It reveals that we need to minimize (3.7) using k_c , not k_h . The cost function of (3.7) can be written as

$$J_{ds} = \frac{\mathbf{c}^T \Lambda_{k_{ref}}^2 \mathbf{c}}{\mathbf{c}^T \mathbf{c}} \quad (3.10)$$

where $\Lambda_{k_{ref}}$ is a diagonal weighting matrix defined as

$$\Lambda_{k_{ref}} = \text{diag}[0, 1, \dots, L_c - 1] - k_{ref} \mathbf{I}_{L_c} \quad (3.11)$$

Now using (3.2), we get

$$J_{ds} = \frac{\mathbf{w}^T \mathbf{H}^T \Lambda_{k_{ref}}^2 \mathbf{H} \mathbf{w}}{\mathbf{w}^T \mathbf{H}^T \mathbf{H} \mathbf{w}} \quad (3.12)$$

Noise and filtered signal power at the output of the TEQ can be written respectively as

$$\sigma_q^2 = \mathbf{w}^T \mathbf{R}_u \mathbf{w} \quad (3.13)$$

$$\sigma_{x_f}^2 = \sigma_x^2 \mathbf{w}^T \mathbf{H}^T \mathbf{H} \mathbf{w} \quad (3.14)$$

The cost function to minimize noise power is defined as ratio of the power of filtered noise power and filtered signal and given by

$$\begin{aligned} J_n &= \frac{\sigma_q^2}{\sigma_{x_f}^2} \\ &= \frac{\mathbf{w}^T \mathbf{R}_u \mathbf{w}}{\sigma_x^2 \mathbf{w}^T \mathbf{H}^T \mathbf{H} \mathbf{w}} \end{aligned} \quad (3.15)$$

Finally, the objective function is formulated by coupling the two cost functions of (3.12) and (3.15) via a trade off parameter, α :

$$J \triangleq \alpha J_{ds} + (1 - \alpha) J_n, \quad 0 \leq \alpha \leq 1 \quad (3.16)$$

Hence, the problem is to find optimum TEQ \mathbf{w}_{opt} by minimizing J in (3.16)

$$\begin{aligned} \mathbf{w}_{opt} &= \arg \min_{\mathbf{w}} J \\ &= \arg \min_{\mathbf{w}} \frac{\mathbf{w}^T \mathbf{X} \mathbf{w}}{\mathbf{w}^T \mathbf{Y} \mathbf{w}} \end{aligned} \quad (3.17)$$

$$\text{where} \quad \mathbf{X} = \alpha \mathbf{H}^T \Lambda_{k_{ref}}^2 \mathbf{H} + \frac{(1 - \alpha)}{\sigma_x^2} \mathbf{R}_u \quad (3.18)$$

$$\mathbf{Y} = \mathbf{H}^T \mathbf{H} \quad (3.19)$$

Again, this formulation falls under the category of (2.2).

3.3.2 Optimum TEQ design

From (3.5), it is obvious that we need to know effective impulse response (EIR), \mathbf{c} , to find k_c which in turn requires to solve (3.17) first. So we proceed to iteratively minimize the (3.38) using centroid obtained at the previous iteration as the time reference for the next [6].

At the i th iteration, optimum \mathbf{w}_{opt} is obtained as

$$\mathbf{w}_i = \arg \min_{\mathbf{w}} J |_{k_{ref}(i-1)} \quad (3.20)$$

Note that at the i th iteration, $\Lambda_{k_{ref}}$ in (3.11) present inside the matrix \mathbf{X} in (3.18) is formed using $k_{ref}(i-1)$. Finally, k_{ref} for the i th iteration is set as the centroid of the effective channel using (3.5):

$$\begin{aligned} k_{ref}(i) &= \frac{1}{E_c} \sum_k k c^2(k) \\ &= \frac{\mathbf{c}^T \Upsilon \mathbf{c}}{\mathbf{c}^T \mathbf{c}} \\ &= \frac{\mathbf{w}_i^T \mathbf{H}^T \Upsilon \mathbf{H} \mathbf{w}_i}{\mathbf{w}_i^T \mathbf{H}^T \mathbf{H} \mathbf{w}_i} \end{aligned} \quad (3.21)$$

$$\text{where } \Upsilon = \text{diag}[0, 1, \dots, L_c - 1]$$

The parameter α can be adapted based on the proportionate ratio of delay spread and filtered noise power :

$$\alpha(i) = \frac{\mathbf{w}_i^T \mathbf{H}^T \Lambda_{k_{ref}(i)}^2 \mathbf{H} \mathbf{w}_i}{\mathbf{w}_i^T \mathbf{Z} \mathbf{w}_i} \quad (3.22)$$

$$\text{where } \mathbf{Z} = \mathbf{H}^T \Lambda_{k_{ref}(i)}^2 \mathbf{H} + \frac{1}{\sigma_x^2} \mathbf{R}_u$$

The proposed algorithm is summarized below:

- Precompute \mathbf{Y} of (3.19) and initialize $k_{ref}(0) = k_h$ i.e as centroid of the original channel and $\alpha(0) = 0.5$ (arbitrary choice).
- for $i=1, 2, \dots$ do the following
 1. Compute the weighting matrix $\Lambda_{k_{ref}}$ of (3.11) using $k_{ref}(i-1)$.
 2. Compute the matrix \mathbf{X} of (3.18) and obtain optimum TEQ for i th iteration, \mathbf{w}_i solving (3.20).
 3. Compute $k_{ref}(i)$ using (3.21).

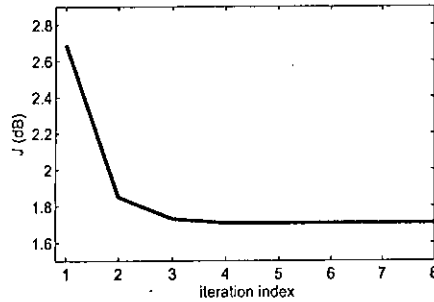


Fig. 3.2: Cost function J gradually stabilizes with iterations (for CSA loop 8).

4. Compute $\alpha(i)$ using (3.22). Here, $\Lambda_{k_{ref}}$ is calculated using $k_{ref}(i)$ as it is available.

Within few iterations, k_{ref} gets locked and J ceases to be minimized more. Then iteration is stopped and w_{opt} is obtained. Fig. (3.2) shows that J cannot increase from iteration to iteration. It is obvious because when k_{ref} is set to k_c (see (3.9)), J_{ds} will minimize which effectively minimizes J as the true time reference is gradually reached with iterations.

3.3.3 Simulation results

Now let us proceed to analyze how the design works. The channels used are eight standard downstream carrier service area (CSA) loops. Configuration of the channels are described in appendix B. A fifth-order Chebyshev highpass filter with cutoff frequency of 4.5 kHz and passband ripple of 0.5 dB is added to each CSA loop to take into account the effect of the splitter at the transmitter. The DC channel, channels 1-3, and the Nyquist channel are not used. This work used the following ADSL input parameters:

- DFT size, $N = 512$ and sampling frequency, $fs = 2.208$ MHz.
- $\nu = 32$, $L_w = 16$ and $L_h = 512$.
- Input power, $\sigma_x^2 = 21$ dBm. Input signal x_k consists of QAM symbols.
- Input noise consists of near-end crosstalk (NEXT) noise plus additive white noise with power density -110 dBm/Hz.

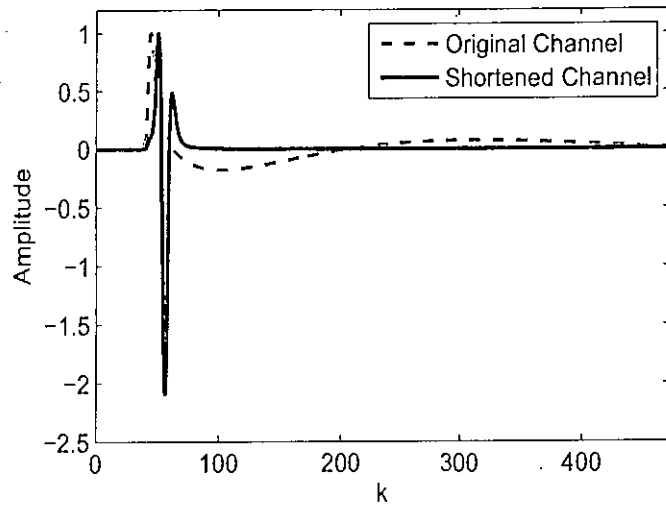


Fig. 3.3: Original and shortened channel impulse responses (for CSA loop 8).

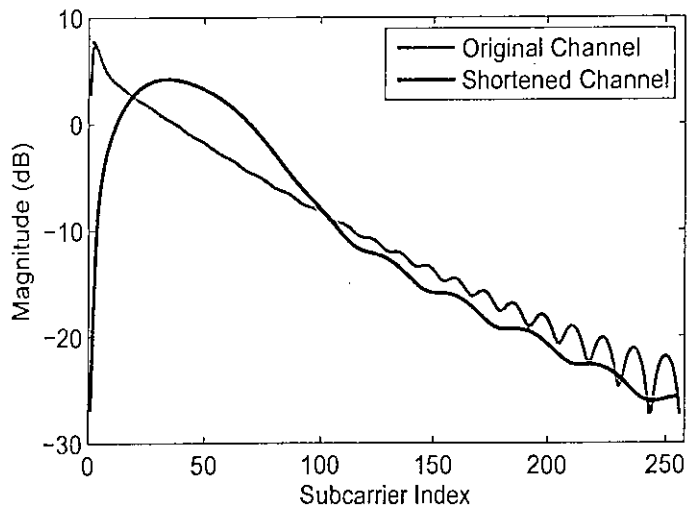


Fig. 3.4: Original and shortened channel frequency responses (for CSA loop 8).

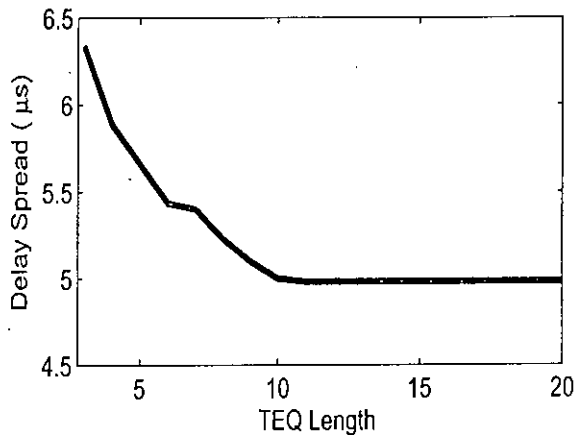


Fig. 3.5: Variation of the delay spread as function of TEQ length (for CSA loop 1).

Fig. (3.3) shows the original and equalized channel impulse responses upto 470 samples for CSA loop no. 8 designed using the proposed method . As one can see, proposed method shortened the channel quite well. Fig. (3.4) shows the corresponding magnitude responses of original and shortened channel. As the cost function jointly minimize delay spread and filtered noise, Figs. (3.5) and Fig. (3.6) show delay spread and output SNR variation as function of TEQ length, L_w . Signal-to-noise ratio (SNR) at the output of the equalizer can be obtained using (3.13) and (3.14) as

$$\begin{aligned}
 \text{SNR} &= \frac{\sigma_{x_f}^2}{\sigma_q^2} \\
 &= \frac{\sigma_x^2 \mathbf{w}^T \mathbf{H}^T \mathbf{H} \mathbf{w}}{\mathbf{w}^T \mathbf{R}_u \mathbf{w}}
 \end{aligned} \tag{3.23}$$

As expected, increasing L_w results in improved performance (delay spread reduces, output SNR rises), which comes at the expense of the increased complexity in implementing the additional equalizer taps. It is also noticed from Figs. (3.5) and (3.6), delay spread and output SNR reaches a floor with increasing L_w . In Table 3.2, the proposed method is compared with other existing methods on the basis of delay spread. Except [6], the proposed method achieves a delay spread that is lower than other methods. Minimum delay spread attained by modified MDS method in [6] is expected as it corrects the original time reference problem

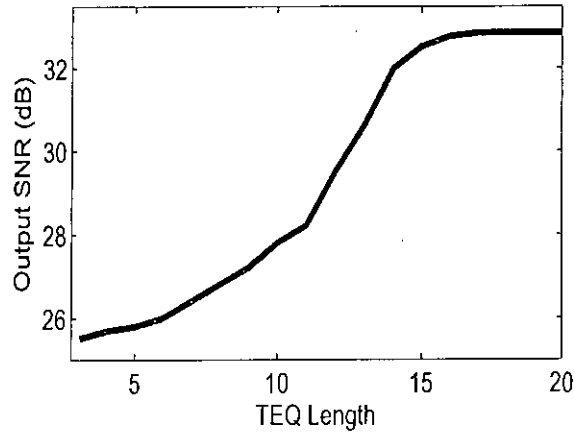


Fig. 3.6: Equalizer output SNR as function of TEQ length (for CSA loop 1).

Table 3.2: Observed delay spread for various methods (averaged over eight CSA loops)

Method	Delay Spread (μ s)
MDS Design [5]	6.27
Eigenfilter Method [2]	7.61
MSSNR Method [4]	4.50
Modified MDS Design [6]	4.40
MMSE Method [3]	4.64
Proposed	4.42

Table 3.3: Output SNR (in dB) comparison of various delay spread minimizing methods

CSA loop no.	MDS [5]	Eigenfilter [2]	Modified MDS [6]	Proposed
1	26.94	22.01	29.31	32.91
2	28.05	20.75	27.10	28.63
3	26.27	20.82	28.91	31.81
4	27.27	18.35	28.00	31.56
5	26.30	21.57	29.10	31.54
6	24.55	19.15	27.87	30.29
7	27.05	17.49	29.81	32.57
8	24.54	15.08	30.01	31.49

Table 3.4: Bit rate comparison with [6]

CSA loop no.	Modified MDS [6]	Proposed
1	2.34	2.46
2	2.05	2.21
3	2.45	2.55
4	1.97	2.15
5	2.21	2.25
6	2.55	2.71
7	2.31	2.41
8	2.43	2.60

present in [5] and only targets to minimize the delay spread. On the other hand, the proposed method performs a trade-off between minimizing delay spread and minimizing noise power. Table 3.3 compares output SNR for the methods which are derived from [5]. It is clear from Table 3.3 that the proposed method achieves higher SNR than those of other methods. Incorporation of α allows appropriate weight for J_{ds} and J_n , so that both the output noise and delay spread are minimized in optimum manner. From Table 3.4, we observe that proposed method outperforms [6] in terms of bit rate. For calculation of bit rate, optimum delay is obtained following (3.40).

3.4 Improved eigenfilter based TEQ design method

It is reported in [25] that two constraints need to be met by TEQs for good throughput performance: 1) the amplitude response associated with the shortened impulse response (SIR) shall have no spectral nulls (if original channel is free of spectral nulls); and 2) the SIR memory need to be shorter than a predefined CP length.

Several methods proposed so far for the design of TEQs fall under the category of eigenfilter design method [3], [4], [19], [5], [25], [2]. Minimum mean-squared error (MMSE) TEQ design method proposed in [3] minimizes the time-domain error between the TEQ output and a desired output, i.e. the output of an FIR filter of order ν . Another design technique called the MSSNR method [4] attempts

to maximize the shortening signal-to-noise ratio (SSNR), where the SSNR is defined as the ratio of energy inside a target window to the energy outside the window. Min-ISI method proposed in [19] partitions the SIR into signal path, ISI path and noise path. This method is shown to achieve higher bit rate than those reported in [3], [4], [5], [25] but it is computationally more complex [11]. In general, MMSE, MSSNR and Min-ISI methods, though shorten the channel well, introduce spectral nulls, thereby not satisfying the aforementioned criteria [25] [include criteria in the introduction]. In [5], a computationally less extensive technique called minimum delay spread (MDS) method is presented which minimizes the delay spread of the effective channel. In [2], a low complexity eigenfilter method is presented which modified the MDS method incorporating cyclic prefix length and effects due to noise. The eigenfilter method (termed as EIGFILT method) proposed in [2] is shown to achieve near optimal bit rate performance. Though [2] requires Cholesky factor computation only once, this method also generates spectral nulls which hinders some potential subcarriers to carry bits.

In this section, the EIGFILT method is modified on different aspects. A new objective function is proposed which explicitly attempts to remove the spectral nulls in the frequency response of the shortened channel. Apart from minimizing residual power of SIR and filtered noise power, delay spread minimization of the desired portion of SIR with respect to a suitable time reference is incorporated to ensure that frequency response flattens to remove spectral nulls and hence allows to transmit more data over the useful signal spectrum. Delay dependent matrices in the proposed method can be updated for each transmission delay Δ following the guidelines of [26] which further reduces computational burden. This work also proposes a heuristic choice of optimum transmission delay which not only allows solving generalized eigenvector (EV) problem only once for TEQ design but also yields profitable bit rate performance.

3.4.1 The EIGFILT method

Consider the model in Fig. 3.1. The method in [2] attempts to optimize the TEQ to shorten the effective channel $c(k)$ and minimizes the filtered noise power σ_q^2 with respect to the filtered signal power $\sigma_{x_f}^2$, where $x_f(k) \triangleq x(k) * c(k)$. The

objective function is given by

$$J_{eig} \triangleq \alpha J_{short} + (1 - \alpha) J_{noise}, \quad 0 \leq \alpha \leq 1 \quad (3.24)$$

where J_{short} and J_{noise} are defined as follows:

$$J_{short} \triangleq \frac{\sum_k f(k - \Delta) |c(k)|^2}{\sum_k |c(k)|^2} \quad (3.25)$$

$$J_{noise} \triangleq \frac{\sigma_q^2}{\sigma_{x_f}^2} = \frac{\sigma_q^2}{\sigma_x^2 \sum_k |c(k)|^2} \quad (3.26)$$

Here J_{short} and J_{noise} are, respectively, the channel shortening and noise suppression objective functions, and α is a trade-off parameter. The penalty function $f(k)$ is formulated as

$$f(k) \triangleq \begin{cases} 0, & 0 \leq k \leq \nu \\ 1, & \text{otherwise.} \end{cases} \quad (3.27)$$

The penalty function penalizes uniformly samples outside $k \in [\Delta, \Delta + \nu]$ where $\Delta \in [0, L_c - \nu - 1]$. For each Δ , the optimum TEQ obtained by the EIGFILT method is obtained as

$$\mathbf{w}_{eig, \Delta} = \underset{\mathbf{w}}{\operatorname{argmin}} J_{eig} \quad (3.28)$$

Delay parameter Δ is varied over the useful range and the optimum delay is chosen for the best bit rate.

3.4.2 Development of a new objective function

The aforementioned method has been proposed to lower the computational cost, especially for the Cholesky factor computation. But unfortunately [2] does not have any control over the frequency response of the TEQ. Optimal TEQ obtained by this method has deep nulls in the frequency domain. Those subchannels with deep nulls become useless. As a result, the presence of these nulls in the magnitude response of the shortened channel reduces the total achievable bit rate of the DMT systems. If the equalizer design problem can incorporate a technique for eliminating these nulls in addition to the channel shortening, it would be possible to achieve much higher bit-rate. In this section, a proposal is presented to achieve this goal.

Similar to approaches in [4] and [19], here the effective channel response \mathbf{c} is divided into two parts—desired portion \mathbf{c}_{des} and residue portion \mathbf{c}_{res} . The proposed objective function comprises the following goals:

1. Minimize the energy of the residual portion \mathbf{c}_{res} to minimize ISI.
2. Minimize the delay spread of the desired portion \mathbf{c}_{des} with respect to a time reference so that it approaches a delta function. This is to ensure flat frequency response and thus to avoid encountering nulls.
3. Minimize noise power σ_q^2 .

Now, we will proceed to develop the proposed objective function. We define two diagonal window matrices, each of size $L_c \times L_c$, to separate the desired and residue portion of the effective channel \mathbf{c} for a particular Δ as

$$\mathbf{G}(\Delta) \triangleq \text{diag}[\mathbf{0}_{1 \times \Delta}, \mathbf{1}_{1 \times (\nu+1)}, \mathbf{0}_{1 \times (L_c - \Delta - \nu - 1)}] \quad (3.29)$$

and

$$\mathbf{D}(\Delta) \triangleq \mathbf{I}_{L_c} - \mathbf{G}(\Delta) \quad (3.30)$$

The residual and desired portion of the channel can be expressed, respectively, as

$$\mathbf{c}_{res} = \mathbf{D}(\Delta)\mathbf{H}\mathbf{w} \quad (3.31)$$

and

$$\mathbf{c}_{des} = \mathbf{G}(\Delta)\mathbf{H}\mathbf{w} \quad (3.32)$$

Then the cost function for minimizing the residual energy can be written as

$$J_{res} \triangleq \frac{\mathbf{c}_{res}^T \mathbf{c}_{res}}{\mathbf{c}^T \mathbf{c}} = \frac{\mathbf{w}^T \mathbf{H}^T \mathbf{D}^2(\Delta) \mathbf{H} \mathbf{w}}{\mathbf{w}^T \mathbf{H}^T \mathbf{H} \mathbf{w}} \quad (3.33)$$

To achieve goal-2, this approach introduces the following cost function for minimizing delay spread within the window with respect to a time reference k_n . This will penalize the desired portion \mathbf{c}_{des} if it deviates from the shape of the delta function.

$$\begin{aligned} J_{des} &\triangleq \frac{1}{E_c} \sum_{k=\Delta}^{\Delta+\nu} (k - k_n)^2 |c_{des}(k)|^2 \\ &= \frac{1}{E_c} \sum_{k=\Delta}^{\Delta+\nu} (k - k_n)^2 |c(k)|^2 \end{aligned} \quad (3.34)$$

where E_c is the energy of effective channel. Here, k_n is taken as the mid-position of the window. Hence, from (3.34) one gets

$$J_{des} = \frac{\mathbf{c}^T \mathbf{\Lambda}^2(\Delta) \mathbf{c}}{\mathbf{c}^T \mathbf{c}} = \frac{\mathbf{w}^T \mathbf{H}^T \mathbf{\Lambda}^2(\Delta) \mathbf{H} \mathbf{w}}{\mathbf{w}^T \mathbf{H}^T \mathbf{H} \mathbf{w}} \quad (3.35)$$

where

$$\Lambda(\Delta) = \text{diag} \left[\underbrace{0, \dots, 0}_{\Delta \text{ zeros}}, \overbrace{\Delta, \Delta + 1, \dots, \Delta + \nu}^{L_c \text{ elements}}, 0, \dots, 0 \right] - k_n \mathbf{G}(\Delta) \quad (3.36)$$

The cost function to minimize noise power at the output of the TEQ is defined as

$$J_{noise} \triangleq \frac{\mathbf{w}^T \mathbf{R}_u \mathbf{w}}{\sigma_x^2 \mathbf{w}^T \mathbf{H}^T \mathbf{H} \mathbf{w}} \quad (3.37)$$

Apparently, it might seem that if goal-2 is satisfied then goal-1 would be automatically ensured. However, a closer inspection would suggest that satisfying goal-2 may not necessarily minimize the residual energy— which is the main target of channel shortening. Clearly, trade-off parameters among these objectives are required for optimum solution. Defining α and β as two trade-off parameters, final objective function can be written as

$$J \triangleq \beta J_{res} + (1 - \alpha - \beta) J_{des} + \alpha J_{noise} \quad (3.38)$$

3.4.3 Optimum TEQ design

For each Δ , optimum TEQ for the proposed method can be obtained by minimizing J , i.e.,

$$\mathbf{w}_\Delta = \underset{\mathbf{w}}{\text{argmin}} J = \underset{\mathbf{w}}{\text{argmin}} \frac{\mathbf{w}^T \mathbf{X} \mathbf{w}}{\mathbf{w}^T \mathbf{Y} \mathbf{w}} \quad (3.39)$$

where

$$\begin{aligned} \mathbf{X} &= \beta \mathbf{H}^T \mathbf{D}^2(\Delta) \mathbf{H} + (1 - \alpha - \beta) \mathbf{H}^T \Lambda^2(\Delta) \mathbf{H} + \frac{\alpha}{\sigma_x^2} \mathbf{R}_u \\ \mathbf{Y} &= \mathbf{H}^T \mathbf{H} \end{aligned}$$

This formulation complies with (2.2). Here \mathbf{Y} is independent of delay and Cholesky factorization for \mathbf{Y} has to be calculated only once over the possible range of Δ . \mathbf{w}_Δ will be the generalized eigenvector corresponding to the smallest generalized eigenvalue of the matrix pair (\mathbf{X}, \mathbf{Y}) for the particular Δ (See appendix A for detail decomposition). Delay parameter Δ is varied and final TEQ \mathbf{w}_{opt} is obtained for Δ_{opt} which yields the maximum bit rate. Fig. 3.7 shows the original channel and SIR by the proposed method for $\Delta_{opt} = 23$, $L_w = 17$, $\nu = 32$, $\alpha = 0.399$ and $\beta = 0.6$ (up to 200 samples shown). Higher value of β is

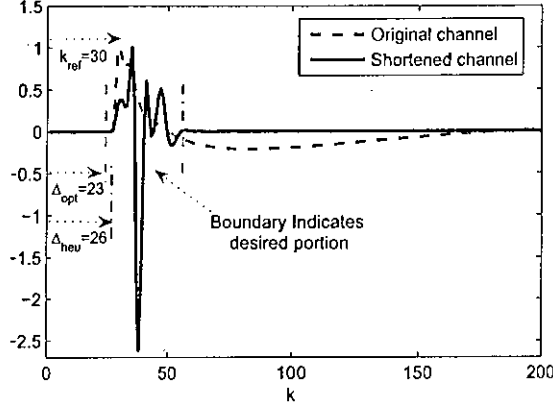


Fig. 3.7: Original and equalized channel impulse responses for CSA loop no. 1. Location of k_{ref} and Δ_{heu} are shown for that channel.

used to set higher priority for suppression of residual portion. Now, residual and desired portion of \mathbf{H} , $\mathbf{H}_{res} = \mathbf{D}(\Delta)\mathbf{H}$ and $\mathbf{H}_{des} = \mathbf{G}(\Delta)\mathbf{H}$, respectively, can be updated for each Δ easily by following [26] which will significantly reduce the complexity of solving generalized EV problem for all Δ values. For example, computing $\mathbf{A}(\Delta) = \mathbf{H}_{res}^T \mathbf{H}_{res}$ from $\mathbf{A}(\Delta - 1)$ requires only $L_w(L_w + \nu)$ multiply and accumulations (MACs) against $L_w^2(L_h - \nu)$ MACs required to compute $\mathbf{A}(\Delta)$ each time.

3.4.4 Heuristic choice of optimum Δ

How to find the optimum Δ without tracing its whole range is still an open problem for delay optimized TEQ design methods. Here, this work proposes a criteria for choosing a heuristic Δ for which bit rate performance is roughly between that of [2] and the proposed method. The heuristic choice is based on the proportion of energy distribution on either side of a particular time reference k_{ref} of the original channel. In this work, we consider index of the maximum value of channel vector \mathbf{h} as the time reference k_{ref} . Defining $E_i \triangleq \sum_{k=0}^{k_{ref}-1} h^2(k)$ and $E_r \triangleq \sum_{k=k_{ref}+1}^{L_h-1} h^2(k)$, heuristic Δ can be obtained as (see Fig. 3.7)

$$\Delta_{heu} = k_{ref} - \left[\frac{E_i(\nu + 1)}{E_i + E_r} \right]^+ \quad (3.40)$$

where $[.]^+$ denotes rounding operation. See Fig. 3.8 for illustration. Performance for this choice of Δ is examined in next section.

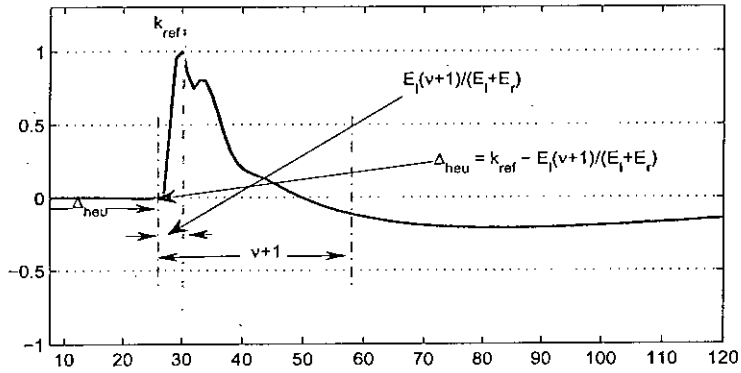


Fig. 3.8: Illustration of heuristic delay Δ_{heu} .

3.4.5 Experimental results

We now proceed to analyze how the design method compares with [2]. As the literature appears to be moving towards the goal of perpetually increasing the bit rate, we opted to compare on the basis of achievable bit rate. The channels used are eight standard downstream CSA loops commonly used in ADSL system simulation (obtained from [24]). Chebyshev highpass filter characteristics are same as that used for the simulation of previous method. The DC channel, channels 1-3, and the Nyquist channel are not used. To make it self-explanatory, ADSL system simulation parameters are listed below again.

- Desired probability of error is 10^{-7} .
- DFT size, $N = 512$ and sampling frequency, $f_s = 2.208\text{MHz}$.
- $\nu = 32$, $L_w = 16$ and $L_h = 512$.
- Input signal $x(k)$ consists of QAM symbols.
- Input power, $\sigma_x^2 = 21$ dBm, SNR gap, $\Gamma = 9.8$ dB (For uncoded QAM constellations, $\Gamma = 9.8$ dB for a symbol error probability of 10^{-7})
- Input noise consists of near-end crosstalk (NEXT) noise plus additive white noise with power density -110 dBm/Hz.

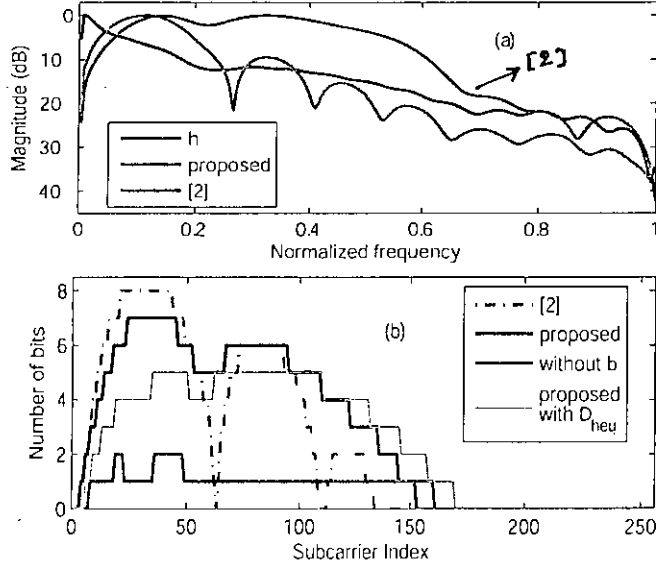


Fig. 3.9: Frequency response of original and equalized channel in (a) and bit allocation over subcarriers in (b) for TEQ designed by the method in [2] and the proposed method, respectively, for CSA loop no. 1.

As the input consists of two-dimensional QAM symbols, the number of bits to allocate in the i th subchannel is [27],

$$b_i = \left\lfloor \log_2 \left(1 + \frac{\text{SNR}_i}{\Gamma} \right) \right\rfloor, \quad 0 \leq i \leq N - 1 \quad (3.41)$$

with $\Gamma = 9.8$ dB here. Here, $\lfloor \cdot \rfloor$ indicates floor operation. We assume that the subchannels are mutually isolated from each other and sufficiently narrowband. SNR_i is taken as the ratio of desired signal power to residual plus noise power on subcarrier i [19]. From this, the bit rate R_b was calculated using,

$$R_b = \frac{f_s}{N + \nu} \sum_i b_i \quad \text{bps} \quad (3.42)$$

In Figs. 3.9(a) and 3.9(b), original and equalized channel frequency response and the corresponding bit allocation into different subcarriers are shown, respectively. From Fig. 3.9(a), it is clear that the channel equalized by the EIGFILT method in [2] contains several nulls in the useful signal band whereas the proposed method eliminates those nulls. Thus the proposed method increases the possibility of achieving higher bit rate by allowing more subcarriers to carry bits by flattening the frequency response in the useful signal band. From Fig. 3.9(b), we notice

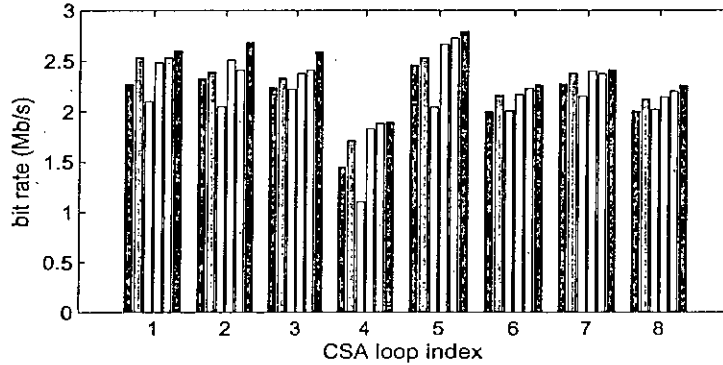


Fig. 3.10: Observed bit rate for CSA loops no. 1-8 using various TEQ design methods. From left to right, height of the bars for each CSA loop denote bit rate obtained by MMSE-UEC [3], MSSNR [4], MDS [5], eigenfilter [2], proposed method with and without Δ_{heu} , respectively.

that shortened channel by EIGFILT method cannot carry data bits in potential subcarriers like 63,109-112 etc. due to attenuation. Moreover, the proposed method not only makes those subcarriers useful but also lets more subcarriers (up to 154, which is 134 for [2]) to carry bits. In Fig. 3.9(b), we see that the proposed method with Δ_{heu} achieves better performance as well.

To emphasize the importance of using two trade-off parameters, the bit allocation for shortened channel obtained by optimizing $J = \alpha(J_{res} + J_{des}) + (1 - \alpha)J_{noise}$ is also plotted instead of (3.38) (i.e., without using β). As different weighting is performed for desired and residual portion, single trade-off parameter cannot successfully adjust suitable weighting between noise and shortening objective functions. Without using β , bit rate comes down as low as 0.65 Mbps for CSA loop no. 1. In Fig. 3.10, comparative achievable bit rate performance of the proposed method with some existing low complexity methods are shown for CSA loops no. 1-8. Achievable bit rates for each method is computed using (3.42). For each method considered except MDS method [5], we varied the delay parameter Δ and chose the value that yielded the best bit rate. From Fig. 3.10, it is clear that the proposed method achieves higher bit rate than all other methods. Like MDS and EIGFILT method, the proposed method also requires only one Cholesky factor computation (for \mathbf{Y} in (3.39)) for all Δ values. From Fig. 3.10, we see that the proposed method using Δ_{heu} performs better than all other methods in most of the occasions. Note that the proposed method using Δ_{heu} requires generalized

EV problem solving only once. With that significant computational advantage, bit rate performance for Δ_{heu} can be considered profitable.

3.5 Iterative MSSNR method

The MSSNR method [4] attempts to minimize ISI in the time domain. The drawbacks of the MSSNR TEQs proposed in [4] include computational sensitivity to transmission delay Δ , inability to design TEQs longer than $\nu + 1$, sensitivity to the fixed point computation in the Cholesky decomposition (which depends on Δ in [4]) and spectral nulls. In this section, we propose an iterative MSSNR design which avoids these limitations and gives shortening performance very close to the direct MSSNR design but with improved bit rate performance.

3.5.1 Modified MSSNR cost function

In [4], MSSNR design works by minimizing the energy outside the target window while holding the energy inside the target window fixed. Using notations from equation (2.7),

$$\mathbf{w}_{opt} = \underset{\mathbf{w}}{\operatorname{argmin}} J = \underset{\mathbf{w}}{\operatorname{argmin}} \frac{\mathbf{w}^T \mathbf{Y} \mathbf{w}}{\mathbf{w}^T \mathbf{X} \mathbf{w}}$$

i.e., minimize $\mathbf{w}^T \mathbf{Y} \mathbf{w}$ while constraining $\mathbf{w}^T \mathbf{X} \mathbf{w} = 1$. When, $L_w > \nu$, \mathbf{X} becomes singular and $(\sqrt{\mathbf{X}})^{-1}$ does not exist (which is required for Cholesky decomposition, See appendix A). Regardless of the choice of L_w , it can be verified [17] that $(\sqrt{\mathbf{Y}})^{-1}$ always exists when the physical channels are copper twisted-pairs (TP) channels. Hence, formulation given in (2.2) applies perfectly for MSSNR to resolve TEQ length problem. For convenience, we restate the formulation here, as it is the basis for development of iterative algorithm.

$$\mathbf{w}_{opt} = \underset{\mathbf{w}}{\operatorname{argmax}} J = \underset{\mathbf{w}}{\operatorname{argmax}} \frac{\mathbf{w}^T \mathbf{X} \mathbf{w}}{\mathbf{w}^T \mathbf{Y} \mathbf{w}}$$

But, as stated earlier, solving the optimization problem over useful range of delays require Cholesky factor computation of \mathbf{Y} for each delay. Replacing $\mathbf{Y} = \mathbf{H}_{res}^T \mathbf{H}_{res}$ by $\mathbf{Y} = \mathbf{H}^T \mathbf{H}$ solves the problem, as $\mathbf{H}^T \mathbf{H}$ does not depend on delay. This design will target to maximize energy inside target window while keeping the total energy fixed to 1. Another parallel design (given below) can be

formulated which attempts to minimize energy outside the window while keeping total energy fixed at 1. (See appendix A for clarification)

$$\mathbf{w}_{opt} = \underset{\mathbf{w}}{\operatorname{argmin}} J = \underset{\mathbf{w}}{\operatorname{argmin}} \frac{\mathbf{w}^T \mathbf{Y} \mathbf{w}}{\mathbf{w}^T \mathbf{X} \mathbf{w}}$$

where, $\mathbf{Y} = \mathbf{H}_{res}^T \mathbf{H}_{res}$ and $\mathbf{X} = \mathbf{H}^T \mathbf{H}$.

3.5.2 Development of iterative MSSNR design

Therefore, the cost function for minimizing the energy in the residue portion can be written as

$$J_{res} = \frac{\mathbf{w}^T \mathbf{Y} \mathbf{w}}{\mathbf{w}^T \mathbf{X} \mathbf{w}} \quad (3.43)$$

For, iterative solution, we define the cost function as

$$J_{res}(n) = \mathbf{w}^T(n) \mathbf{Y} \mathbf{w}(n) \quad (3.44)$$

Here, n denotes iteration index. The performance surface is quadratic and method of steepest descent can be readily implemented. The gradient $\nabla J_{res}(n)$ can be evaluated as

$$\nabla J_{res}(n) = (\mathbf{Y} + \mathbf{Y}^T) \mathbf{w}(n) \quad (3.45)$$

which results in the gradient descent update equation as

$$\mathbf{w}(n+1) = \mathbf{w}(n) - \mu \nabla J_{res}(n) \quad (3.46)$$

Here, μ is the step size that governs the stability and convergence speed of the algorithm. The constraint $\mathbf{w}^T \mathbf{X} \mathbf{w}$ should also be incorporated [28], which can be implemented by renormalizing $\mathbf{w}(n)$ after each iteration, i.e.,

$$\mathbf{w}(n+1) = \frac{\mathbf{w}(n+1)}{\sqrt{\mathbf{w}^T(n+1) \mathbf{X} \mathbf{w}(n+1)}} \quad (3.47)$$

The expensive renormalization in (3.47) can be avoided through the use of a Lagrangian constraint following [29].

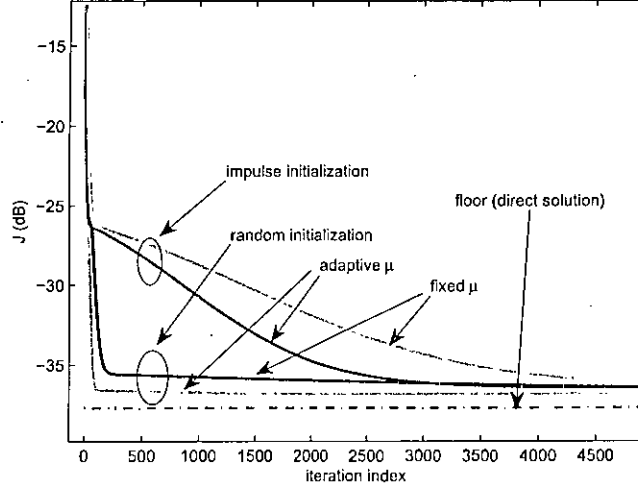


Fig. 3.11: Performance of iterative MSSNR algorithm for CSA loop no. 8. Two kinds of initialization used: a) random and b) impulse.

3.5.3 Step size adaptation

Now, this work proposes a variable step size that ensures optimal performance and speedy convergence of the adaptation process. We define a cost function as

$$J_{\mu}(n) = [\mathbf{w}_{opt} - \mathbf{w}(n+1)]^T [\mathbf{w}_{opt} - \mathbf{w}(n+1)] \quad (3.48)$$

Minimizing $J_{\mu}(n)$ ensures the minimum distance between $\mathbf{w}(n+1)$ and \mathbf{w}_{opt} at each iteration. Substituting (3.46) into (3.48) and setting $\partial J_{\mu}(n)/\partial \mu(n) = 0$, we obtain the expression for variable step size as

$$\mu_{adap}(n) = \frac{\nabla J_{res}^T(n) [\mathbf{w}(n) - \mathbf{w}_{opt}]}{\|\nabla J_{res}(n)\|^2} \quad (3.49)$$

where $\|\cdot\|$ is the l_2 norm. In (3.49), \mathbf{w}_{opt} is unknown. However, it can be easily shown that

$$\nabla J_{res}^T(n) \mathbf{w}_{opt} = \mathbf{w}^T(n) (\mathbf{Y} + \mathbf{Y}^T) \mathbf{w}_{opt} = 0.$$

Therefore, the optimal step size from (3.49) becomes

$$\mu_{adap}(n) = \frac{\nabla J_{res}^T(n) \mathbf{w}(n)}{\|\nabla J_{res}(n)\|^2} \quad (3.50)$$

It is desired that the step size is larger in the initial iterations to allow faster con-

vergence but gradually decreased to reduce the final misalignment error. Therefore we adopt a constraint on the step size such that if estimated $\mu_{adap}(n)$ is greater than $\mu_{adap}(n-1)$, then $\mu_{adap}(n) = \mu_{adap}(n-1)$.

In Fig. 3.11, it is observed that iterative algorithm reaches very close to the floor set by MSSNR algorithm. It is interesting to note that random TEQ initialization performs faster than that with impulse initialization for TEQ. It is because optimum TEQ impulse response is never an impulse, otherwise equalizer output would not change from input. So, random initialization helps to reach optimum level quickly. It is also noticeable that adaptive μ achieves superior performance when compared to fixed μ , as expected. Fixed μ is taken equal to the level to which adaptive μ settles. During first hundreds of iterations, adaptive μ takes larger values which results in faster convergence.

3.5.4 Simulation results

We now proceed to analyze how the design works. The channels used are eight standard downstream carrier service area (CSA) loops. Data for the channel and noise was obtained from the Matlab DMTTEQ Toolbox [24]. This work adds a fifth-order Chebyshev highpass filter with similar characteristics as used before to each CSA loop to take into account the effect of the splitter at the transmitter. The DC channel, channels 1-3, and the Nyquist channel are not used.

In Fig. 3.12, we see that iterative algorithm shortens the channel satisfactorily. Iterative algorithm using adaptive μ almost coincides with original MSSNR design, showing the merit of the proposed approach. It is reported in [18] that finite length MSSNR TEQs are approximately symmetric. As the TEQ length increases, symmetry becomes more prominent and ν zeros get close to unit circle and kills those subcarriers. In Figs. 3.13, 3.14, 3.15, it is obvious that MSSNR design have some deep fade in useful signal band, whereas iterative technique avoids null in those region and allows to utilize more subcarriers.

Table 3.5 shows SSNR performance of direct and iterative MSSNR techniques. Iterative MSSNR with adaptive μ most often come close to direct MSSNR performance. This slight reduction seems profitable when we observe the results in Table 3.6. For all 8 channels, iterative techniques achieve higher bit rate than MSSNR method. As bit rate is the standard performance metric for ADSL

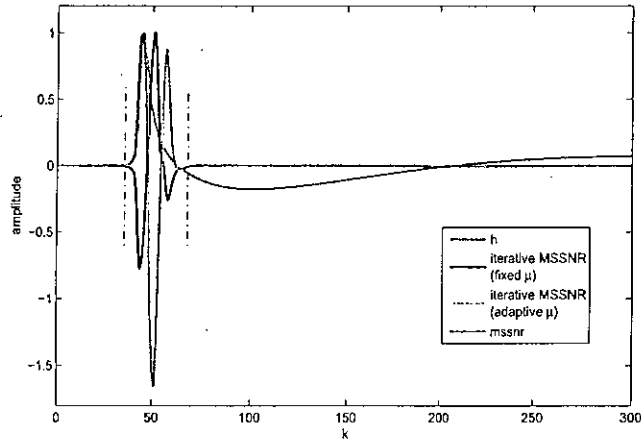


Fig. 3.12: Shortened channel by iterative MSSNR algorithm for CSA loop no. 8 (for random initialization). Shortened channel using adaptive μ almost coincides with direct MSSNR solution.

Table 3.5: Shortening SNR comparison for direct and iterative MSSNR methods. All values in dB.

Channel no.	MSSNR [4]	fixed μ	adaptive μ
1	49.75	37.42	46.02
2	41.97	38.93	40.00
3	57.49	49.11	48.50
4	50.86	37.93	41.25
5	36.17	35.33	36.03
6	58.23	48.64	47.12
7	55.26	37.05	40.08
8	48.53	37.47	41.79

systems, this method has high practical significance with low computational complexity.

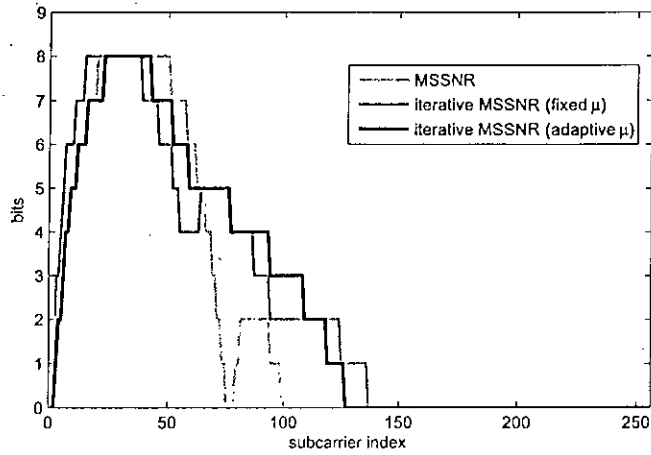


Fig. 3.13: Bit allocation in different subcarriers by iterative algorithm. It is clear that iterative algorithm allows more subcarriers to carry bits (for CSA loop no. 8).

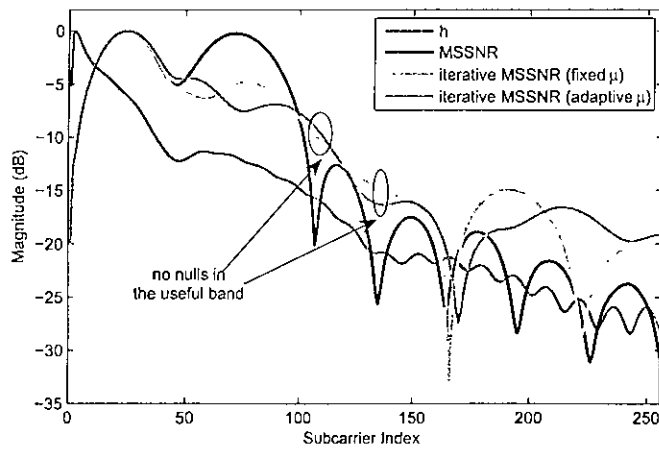


Fig. 3.14: Frequency response of the shortened channel. It is clear that iterative algorithm avoids severe nulls in the useful signal band (for CSA loop no. 7).

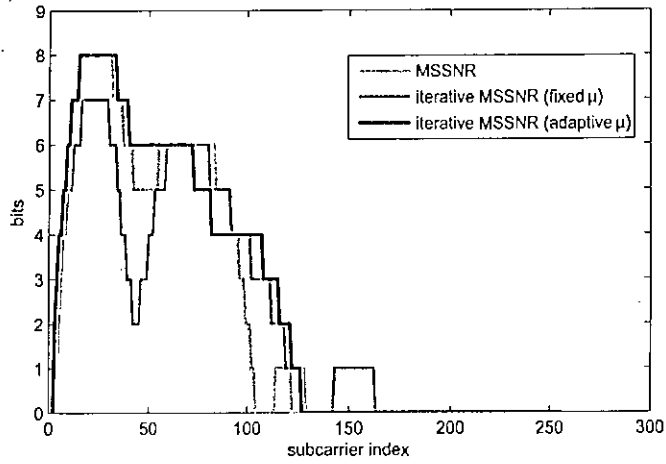


Fig. 3.15: Bit allocation in different subcarriers by iterative algorithm. This figure supports Fig. 3.14 that how more subcarriers can be utilized by iterative method unlike direct MSSNR approach (for CSA loop no. 7).

Table 3.6: Bit rate comparison for direct and iterative MSSNR methods. All values in Mbps.

Channel no.	MSSNR [4]	fixed μ	adaptive μ
1	1.9564	2.4150	2.4353
2	2.3663	2.3135	2.6179
3	1.8589	2.3054	2.4637
4	2.0497	2.6058	2.7356
5	1.6195	2.2364	2.3460
6	1.9929	2.6585	2.9061
7	1.5708	3.1294	3.4500
8	2.4718	2.7032	2.8209

3.6 Conclusion

In this chapter, three adaptive and non-adaptive non-blind TEQ design algorithms are presented. First, MDS method has been modified by incorporating true time reference and noise in the channel, and TEQ is updated by an iterative algorithm. The algorithm converges quickly and obtains satisfactory delay spread and noise performance. Then, an improved eigenfilter method is presented which improved EIGFILT method to account for spectral nulls and obtains bit rate improvement. A heuristic choice of delay is also proposed which significantly minimizes computational burden to run the design over all delays. Finally, MSSNR method is modified and an iterative algorithm is presented to remove the shortcomings of MSSNR method.

Chapter 4

The MIMO channel shortening algorithm

4.1 Introduction

In this chapter, channel shortening for cyclic-prefixed block transmission system over multiple input multiple output (MIMO) channels is considered. Since the channel encountered in traditional DMT system is a SISO channel, most, if not all, design methods for TEQs have been only for SISO channels. For DMT/OFDM modulation, several methods were proposed for the design of TEQs. In [3], Al-Dhahir and Cioffi proposed minimum mean squared error (MMSE) optimal decision feedback equalizer (DFE) training algorithm. Melsa, Younce, and Rohrs proposed MSSNR method which directly minimizes the part of the SIR that causes ISI [4]. This is a more effective method to reduce ISI than the methods based on the MSE. In a MIMO system multiple channels need to be shortened simultaneously. Joint channel shortening can be combined with multiuser detection and precoding to mitigate crosstalk. MIMO channel shortening using a generalized MIMO-MMSE-DFE structure has been studied by Al-Dhahir [30]. Youming in [31] proposed a MIMO channel shortening algorithms which operate in multiple stages to jointly shorten the channels.

In this work, we directly extend the original MSSNR algorithm into the MIMO case. Based on this structure, we successfully develop MSSNR channel shortening method to jointly shorten MIMO ISI channels. The MIMO TEQ is formed with eigenvectors corresponding to some maximum eigenvalues of a particular matrix. This design is suitable for any arbitrary length TEQ [17] as well. The proposed scheme is tested for some common figures of merits such as equalization SNR,

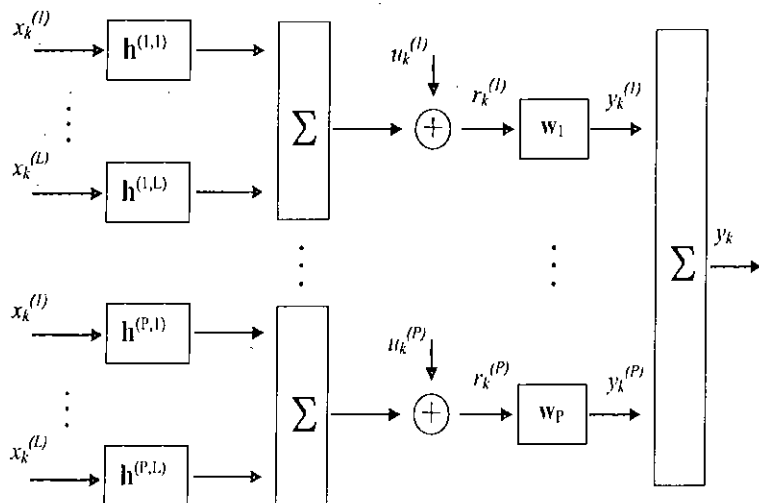


Fig. 4.1: MIMO TEQ model, for L transmit antennas and P receive antennas. Channel $\mathbf{h}^{(p,l)}$ connects the l th transmitter to the p th receiver antenna. $y_k^{(j)}$ denotes k th sample of equalizer output at j th receive antenna.

energy compaction ratio, signal to interference plus noise ratio and obtained good shortening performances compared to [30]. We also proposed a heuristic bit rate formula for MIMO channel shortening systems and compared bit rates with [30], [31] and achieved encouraging results.

4.2 System model

Consider a MIMO communication system with L transmit and P receive antennas. The baseband system model can be written as

$$r_k^{(j)} = \sum_{i=1}^L \sum_{m=0}^{p-1} h_m^{(j,i)} x_{k-m}^{(i)} + u_k^{(j)} \quad (4.1)$$

where $r_k^{(j)}$ is the received signal at the j th antenna for time k , $h_m^{(i,j)}$ is the m th channel tap for the channel between i th transmit antenna and j th receive antenna, $u_k^{(j)}$ is the noise (modeled as white noise) affecting the received signal of the j th receive antenna at time k , and p is the maximum length of all the $L \times P$ channels.

See Fig. 4.1 for illustration. Let at time k ,

$$\begin{aligned} \mathbf{r}_k &= [r_k^{(1)}, r_k^{(2)}, \dots, r_k^{(P)}], \\ \mathbf{x}_k &= [x_k^{(1)}, x_k^{(2)}, \dots, x_k^{(L)}], \\ \mathbf{u}_k &= [u_k^{(1)}, u_k^{(2)}, \dots, u_k^{(P)}] \end{aligned} \quad (4.2)$$

where \mathbf{r}_k , \mathbf{x}_k and \mathbf{u}_k are received signal vector, transmitted signal vector and noise vector respectively. Then in vector form, (4.1) can be written as

$$\mathbf{r}_k = \sum_{m=0}^{p-1} \mathbf{H}_m \mathbf{x}_{k-m} + \mathbf{u}_k \quad (4.3)$$

where \mathbf{H}_m is the MIMO channel matrix coefficient of size $P \times L$. By stacking q samples of the received signal vector, (4.3) can be written as

$$\begin{aligned} \begin{bmatrix} \mathbf{r}_k \\ \mathbf{r}_{k-1} \\ \vdots \\ \mathbf{r}_{k-q+1} \end{bmatrix} &= \begin{bmatrix} \mathbf{H}_0 & \mathbf{H}_1 & \cdots & \mathbf{H}_{p-1} & \mathbf{0} & \cdots & \mathbf{0} \\ \mathbf{0} & \mathbf{H}_0 & \cdots & \mathbf{H}_{p-2} & \mathbf{H}_{p-1} & \ddots & \vdots \\ \vdots & \vdots & \ddots & \vdots & \vdots & \ddots & \vdots \\ \mathbf{0} & \cdots & \cdots & \mathbf{H}_{p-q} & \mathbf{H}_{p-q+1} & \cdots & \mathbf{H}_{p-1} \end{bmatrix} \\ &\times \begin{bmatrix} \mathbf{x}_k \\ \mathbf{x}_{k-1} \\ \vdots \\ \mathbf{x}_{k-p-q+1} \end{bmatrix} + \begin{bmatrix} \mathbf{u}_k \\ \mathbf{u}_{k-1} \\ \vdots \\ \mathbf{u}_{k-q+1} \end{bmatrix} \end{aligned} \quad (4.4)$$

In compact form, (4.4) can be written as

$$\mathbf{r} = \mathbf{H}\mathbf{x} + \mathbf{u} \quad (4.5)$$

where \mathbf{H} is a block Toeplitz matrix of size $Pq \times L(p+q-1)$, \mathbf{r} and \mathbf{u} are $Pq \times 1$ vectors, and \mathbf{x} is a $L(p+q-1) \times 1$ vector.

4.3 Proposed MIMO MSSNR channel shortening

4.3.1 Problem formulation

Given the MIMO channel matrix \mathbf{H} having p matrix taps, the objective is to design a MIMO TEQ, $\mathbf{W} = [\mathbf{W}_0, \mathbf{W}_1, \dots, \mathbf{W}_{q-1}]^T$ of q matrix taps, each of size $P \times L$, to equalize \mathbf{H} to maximize the energy in a window of $d = \nu+1$ matrix taps

of the effective channel matrix, $C_{eff} = \mathbf{H}^T \mathbf{W}$ (of size $L(p+q-1) \times L$) keeping the energy in the remainder of the effective channel fixed.

Let us define two window matrices, each of size $L(p+q-1) \times L(p+q-1)$:

$$\mathbf{G}_\Delta = \begin{bmatrix} \mathbf{0}_{\Delta L} & \mathbf{0} & \mathbf{0} \\ \mathbf{0} & \mathbf{I}_{dL} & \mathbf{0} \\ \mathbf{0} & \mathbf{0} & \mathbf{0}_{(p+q-d-\Delta-1)L} \end{bmatrix} \quad (4.6)$$

$$\overline{\mathbf{G}}_\Delta = \mathbf{I}_{L(p+q-1)} - \mathbf{G}_\Delta \quad (4.7)$$

where Δ is the transmission delay parameter which lies within the range $0 \leq \Delta \leq p+q-d-1$, \mathbf{I}_N denotes the identity matrix of size $N \times N$ and $\mathbf{0}_M$ denotes $M \times M$ zero matrix. Then the desired and residual portion of the channel matrix \mathbf{H} can be defined, respectively, as

$$\mathbf{H}_{des} = \mathbf{H} \mathbf{G}_\Delta \quad (4.8)$$

$$\mathbf{H}_{res} = \mathbf{H} \overline{\mathbf{G}}_\Delta \quad (4.9)$$

Desired and residual portion of effective channel matrix can be given as

$$\mathbf{C}_{des} = \mathbf{H}_{des}^T \mathbf{W} = \mathbf{W}^T \mathbf{B} \mathbf{W} \quad (4.10)$$

$$\mathbf{C}_{res} = \mathbf{H}_{res}^T \mathbf{W} = \mathbf{W}^T \mathbf{A} \mathbf{W} \quad (4.11)$$

Desired signal power at equalizer output is $\sigma_x^2 \text{trace}(\mathbf{C}_{des}^T \mathbf{C}_{des})$ or equivalently $\sigma_x^2 \text{trace}(\mathbf{W}^T \mathbf{B} \mathbf{W})$ and residue signal power at equalizer output is similarly given by $\sigma_x^2 \text{trace}(\mathbf{W}^T \mathbf{A} \mathbf{W})$, where σ_x^2 is the input symbol power, $\mathbf{B} = \mathbf{H}_{des} \mathbf{H}_{des}^T$ and $\mathbf{A} = \mathbf{H}_{res} \mathbf{H}_{res}^T$.

Now, MSSNR problem in MIMO case can be formulated as

$$\mathbf{W}_{opt} = \arg \max_{\mathbf{W}} \text{trace}(\mathbf{W}^T \mathbf{B} \mathbf{W}) \quad \text{s.t.} \quad \mathbf{W}^T \mathbf{A} \mathbf{W} = \mathbf{I}_L \quad (4.12)$$

or equivalently (See appendix A for clarification.)

$$\mathbf{W}_{opt} = \arg \max_{\mathbf{W}} \text{trace}(\mathbf{W}^T \mathbf{C} \mathbf{W}) \quad \text{s.t.} \quad \mathbf{W}^T \mathbf{A} \mathbf{W} = \mathbf{I}_L \quad (4.13)$$

where

$$\mathbf{C} = \mathbf{A} + \mathbf{B} = \mathbf{H} \mathbf{H}^T \quad (4.14)$$

Note that (4.12) and (4.13) will lead to the same TEQ, except that they are different by a amplitude scale factor [32]. But (4.13) will lead to faster TEQ computation as matrix \mathbf{C} is the same for all delays, whereas matrices \mathbf{A} and \mathbf{B} have to be recomputed for each delay. Apart from computational saving, (4.13) works for any value of q as well [17].

4.3.2 Optimum MIMO TEQ design

Assuming \mathbf{A} is positive definite and has full rank of Pq such that $(\sqrt{\mathbf{A}})^{-1}$ exists, \mathbf{A} can be decomposed using Cholesky decomposition into

$$\mathbf{A} = \sqrt{\mathbf{A}}(\sqrt{\mathbf{A}})^T \quad (4.15)$$

Let us define

$$\mathbf{Y} = (\sqrt{\mathbf{A}})^T \mathbf{W} \quad (4.16)$$

Then using (4.13), we obtain

$$\mathbf{Y}^T \mathbf{Y} = \mathbf{W}^T \sqrt{\mathbf{A}} (\sqrt{\mathbf{A}})^T \mathbf{W} = \mathbf{W}^T \mathbf{A} \mathbf{W} = \mathbf{I}_L \quad (4.17)$$

Hence from (4.13) and (4.16), it follows that

$$\mathbf{W}^T \mathbf{C} \mathbf{W} = \mathbf{Y}^T (\sqrt{\mathbf{A}})^{-1} \mathbf{C} (\sqrt{\mathbf{A}}^T)^{-1} \mathbf{Y} = \mathbf{Y}^T \mathbf{Z} \mathbf{Y} \quad (4.18)$$

where

$$\mathbf{Z} = (\sqrt{\mathbf{A}})^{-1} \mathbf{C} (\sqrt{\mathbf{A}}^T)^{-1} \quad (4.19)$$

If we define eigendecomposition of \mathbf{Z} as

$$\mathbf{Z} = \mathbf{U} \mathbf{\Lambda} \mathbf{U}^T = \mathbf{U} \text{diag}(\gamma_0, \gamma_1, \dots, \gamma_{Pq-1}) \mathbf{U}^T \quad (4.20)$$

where $\gamma_0 \geq \gamma_1 \geq \dots \geq \gamma_{Pq-1}$. Then optimal shortening can be considered as choosing \mathbf{Y} to maximize $\mathbf{Y}^T \mathbf{Z} \mathbf{Y}$ constraining $\mathbf{Y}^T \mathbf{Y} = \mathbf{I}_L$. The solution to this problem occurs for $\mathbf{Y}_{opt} = \mathbf{U}[\mathbf{e}_0, \mathbf{e}_1, \dots, \mathbf{e}_{L-1}]$ (\mathbf{e}_i denotes the i th unit vector) which contains L eigenvectors corresponding to the maximum L eigenvalues of \mathbf{Z} . Finally, it follows that

$$\mathbf{W}_{opt} = (\sqrt{\mathbf{A}}^T)^{-1} \mathbf{Y}_{opt} \quad (4.21)$$

Delay parameter Δ present inside \mathbf{A} is optimized to maximize $\text{trace}(\mathbf{D})$, where

$$\mathbf{D} = \text{diag}(\gamma_0, \gamma_1, \dots, \gamma_{L-1}) \quad (4.22)$$

Table 4.1 summarizes the key vectors and matrices used in the algorithm and their sizes.

Table 4.1: Summary of key vectors and matrices used in MIMO channel shortening scheme.

Vectors/Matrices	Name	Size
\mathbf{r}	Received Signal Vector	$Pq \times 1$
\mathbf{x}	Transmitted Signal Vector	$L(p+q-1) \times 1$
\mathbf{u}	Receiver Noise Vector	$Pq \times 1$
\mathbf{H}	Channel Matrix	$Pq \times L(p+q-1)$
\mathbf{W}	TEQ matrix	$Pq \times L$
\mathbf{C}_{eff}	Effective Channel Matrix	$L(p+q-1) \times L$
\mathbf{C}	Defined in Equation (4.14)	$Pq \times Pq$
\mathbf{C}_{des}	Desired portion of \mathbf{C}_{eff}	$L(p+q-1) \times L$
\mathbf{C}_{res}	Residual portion of \mathbf{C}_{eff}	$L(p+q-1) \times L$

4.4 Simulation results

This section presents experimental results of the proposed algorithm. The input and noise processes are assumed to be uncorrelated. Input signal to noise ratio σ_x^2/σ_u^2 is chosen to be 20 dB. Channels are generated as zero mean uncorrelated Gaussian random variables. To test our proposed channel shortening method, we have decided to compare it with MMSE method of [30] for the following figures of merit:

$$\text{Equalization SNR} = \frac{\text{Energy inside window}}{\text{Energy outside window}} = \frac{\text{trace}(\mathbf{W}^T \mathbf{B} \mathbf{W})}{\text{trace}(\mathbf{W}^T \mathbf{A} \mathbf{W})} \quad (4.23)$$

$$\begin{aligned} \text{Energy compaction ratio, } \rho &= \frac{\text{Energy inside window of shortened channel}}{\text{Energy of shortened channel}} \\ &= \frac{\text{trace}(\mathbf{W}^T \mathbf{B} \mathbf{W})}{\text{trace}(\mathbf{W}^T \mathbf{C} \mathbf{W})} \end{aligned} \quad (4.24)$$

Overall Signal to (Interference + Noise) Ratio, SINR

$$\begin{aligned} &= \frac{\text{Desired signal power at o/p of equalizer}}{\text{Residue signal power at o/p of equalizer} + \text{Noise power at o/p of equalizer}} \\ &= \frac{\sigma_x^2 \text{trace}(\mathbf{W}^T \mathbf{B} \mathbf{W})}{\sigma_x^2 \text{trace}(\mathbf{W}^T \mathbf{A} \mathbf{W}) + \sigma_u^2 \text{trace}(\mathbf{W}^T \mathbf{W})} \end{aligned} \quad (4.25)$$

We propose a heuristic bit rate formula for MIMO channel shortening system as

$$\begin{aligned} R &= \log_2 \left(1 + \frac{\text{SINR}}{\Gamma} \right) \quad \text{bits/symbol} \\ &= \frac{F_s}{(N + \nu)} \log_2 \left(1 + \frac{\text{SINR}}{\Gamma} \right) \quad \text{bits/sec} \end{aligned} \quad (4.26)$$

Table 4.2: Achievable bit rate comparison ($\Gamma = 9.8$ dB, $p = 512$, $q = 13$, $\nu = 32$, $N = 512$, $L = 2$, $P = 2$)

Method	Bit rate (Mbps)	
	$L=1, P=1$	$L=2, P=2$
Proposed	5.58	8.67
MMSE [30]	5.61	8.68
Youming's MSSNR [31]	4.43	7.53

where, F_s is the sampling frequency chosen to be 2.208 MHz, N is the IFFT size. $N + \nu$ constitutes the total length of the DMT symbol including CP. Γ is the SNR gap required to achieve a target bit error rate. SINR is computed using (4.25).

In Fig. 4.2, performances of MSSNR and MMSE schemes are compared for equalization SNR as function of delay. It is clear from Fig. 4.2 that MSSNR can achieve higher SNR at the optimum delay than that of MMSE method. In Fig. 4.3, two methods are compared for equalization SNR as function of TEQ length. It shows that MSSNR method achieves good shortening performances for small number of TEQ taps. In Fig. 4.4, two methods are compared for energy compaction ratio, ρ as function of TEQ length. ρ is a very important metric as it gives a measure of how much of the effective channel energy is contained within the desired window of interest. Clearly, $0 \leq \rho \leq 1$ and for efficient channel shortening, a larger ρ is required. Again, we can see MSSNR method gives better result for small number of TEQ taps. In Fig. 4.5, two methods are compared for SINR as function of TEQ length. It is expected that MSSNR will face some performance loss as its output noise power is not considered in the cost function (4.13). Still for some TEQ lengths, SINRs are comparable. Still for some TEQ lengths, SINRs are comparable. For Figs. 4.3 and 4.5, the parameters chosen are $p = 512$, $\nu = 15$, $L = 2$ and $P = 2$.

In Figs. 4.6 and 4.7, joint channel shortening for a 2×2 system is shown with the derived algorithm and MMSE method respectively. Finally, in Table 4.2 the proposed scheme is compared with [30], [31] for achievable bit rate using (4.26) and obtained performances comparable to that of MMSE method but with less computational complexity. When compared to [31], the proposed method achieves higher bit rates.

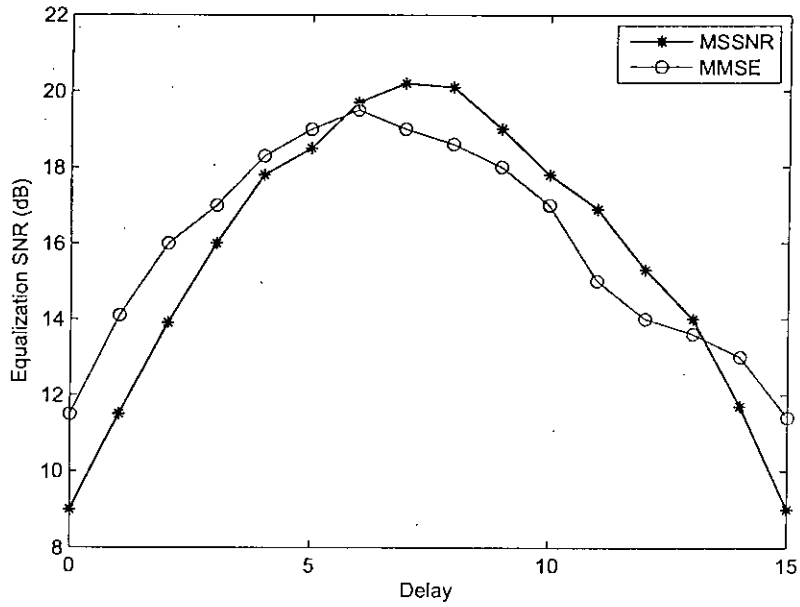


Fig. 4.2: Variation of the equalization SNR of the MIMO TEQ vs delay over 100 channel realizations ($p = 7, q = 12, \nu = 2, L = 2, P = 2$).

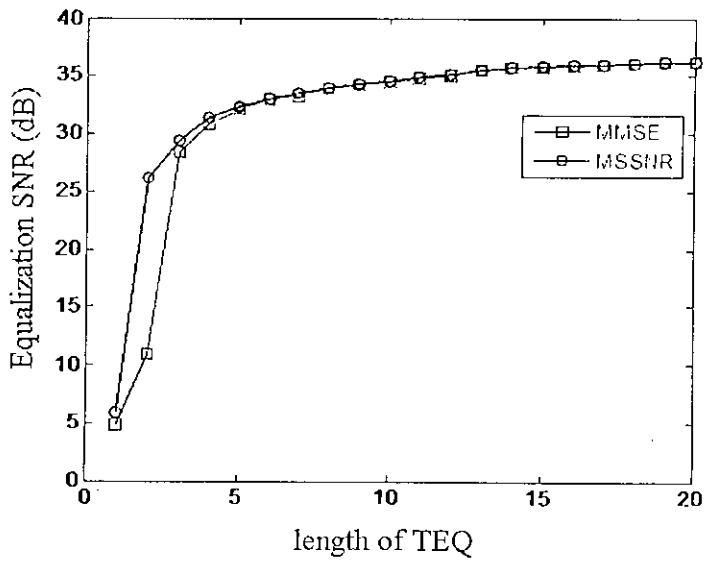


Fig. 4.3: Variation of the equalization SNR as a function of TEQ length.

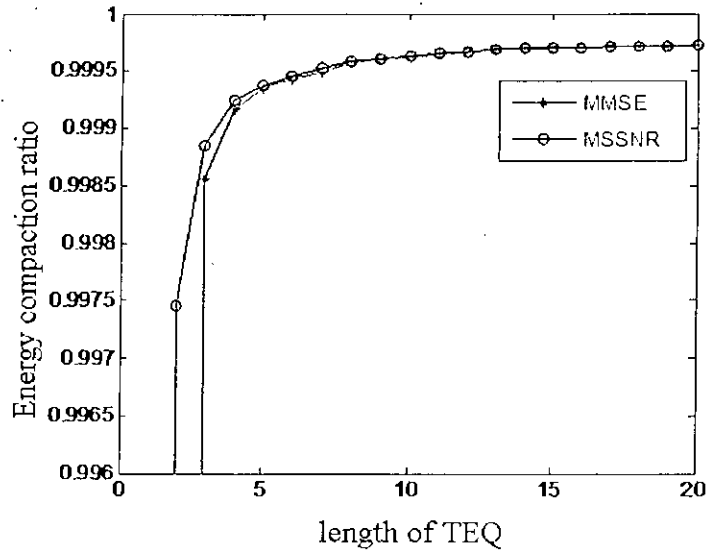


Fig. 4.4: Energy Compaction ratio as a function of TEQ length.

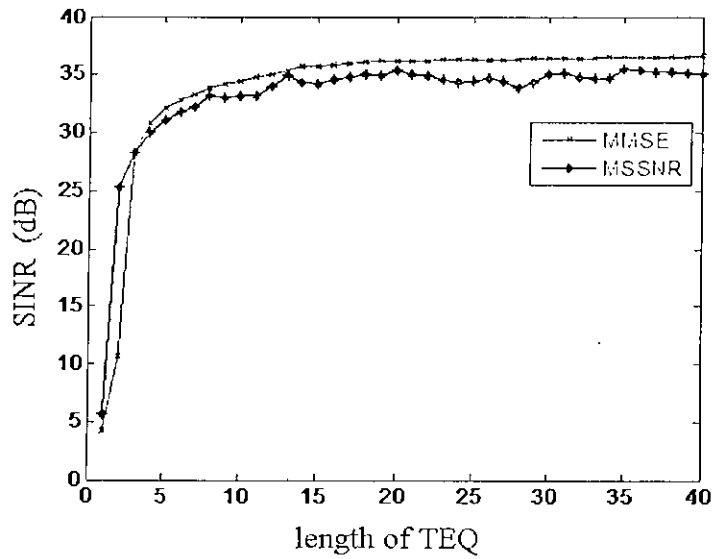


Fig. 4.5: Variation of the SINR as a function of TEQ length.

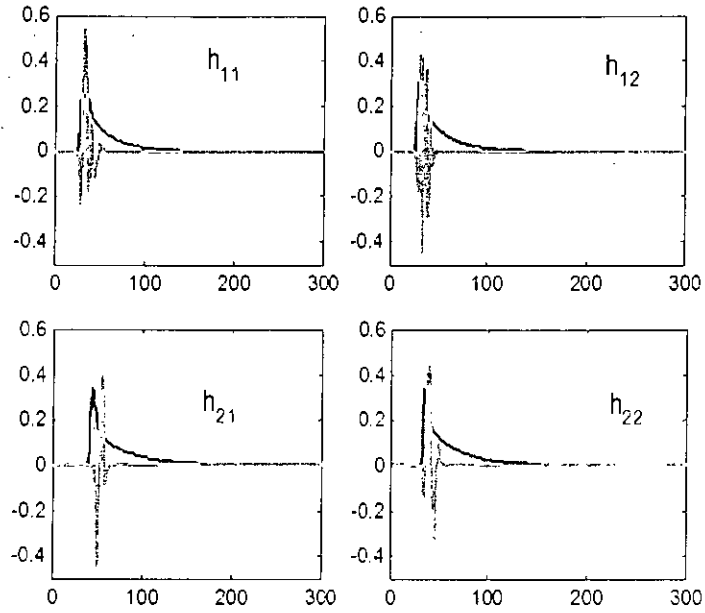


Fig. 4.6: Original and shortened channels($p = 300, q = 13, \nu = 15, L = 2, P = 2$) (MSSNR method).

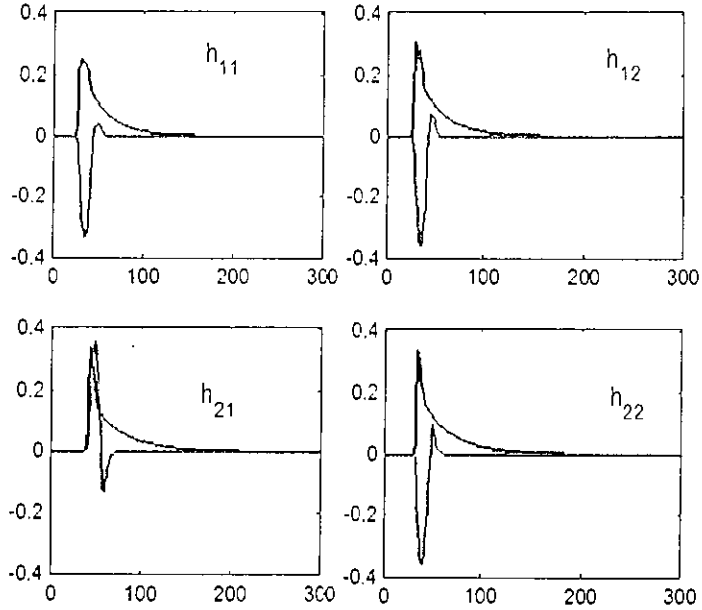


Fig. 4.7: Original and shortened channels($p = 300, q = 13, \nu = 15, L = 2, P = 2$) (MMSE method).

4.5 Conclusion

In this chapter, MIMO channel shortening by maximizing composite shortening SNR is discussed. The extension to the MIMO case is motivated by the simplicity and good channel shortening performance of the MSSNR method for single channel. MIMO MSSNR method achieves best channel shortening performance than other MIMO TEQ design methods. Even MIMO MSSNR algorithm gives SINR and bit rates comparable to MMSE method but at much less computational complexity. The design is adaptable to arbitrary length TEQ as well. Experimental results demonstrate superior performance of the algorithm.

Chapter 5

Conclusion

5.1 Summary

Research and development is continuing to improve the performance of DMT systems for current and future applications and standards. Improvement in TEQ design methods has a potential to increase the achievable bit rates in DMT systems. Combining a TEQ with a guard period (cyclic prefix) is used to prevent inter-symbol interference in DMT transceivers. The TEQ shortens the channel to the length of the guard period so that two adjacent symbols do not interfere with each other.

Many different TEQ design methods have been proposed. Among them, those based on the Minimum Mean Squared Error (MMSE) are the most commonly used in commercial ADSL modems [3]. MMSE design methods are relatively easier to implement with adaptive algorithms and are efficient in the sense of computational complexity. However, MMSE design methods and other reported eigenfilter based methods are not optimal in the sense of maximizing channel capacity as they exhibit spectral nulls in the frequency response, thus hinder some potential subcarriers to carry bits. Hence, the main motivation of this work was to design low complexity TEQ design methods which, along with good channel shortening, do not exhibit spectral attenuation and hence improve bit rate performance. To develop a holistic view of different performance implications, a concise literature survey of some eigenfilter based TEQ design methods were presented along with their shortcomings. This engenders readers to comprehend the claim on performance improvement by different proposed methods in the following chapters.

In Chapter 3, first, a generalization of minimum delay spread design method [5] has been proposed which takes into account the noise observed in DMT systems. An iterative TEQ design method was presented which jointly minimize delay spread of the channel and filtered noise at the output of the equalizer. To attain overall cost function minimization, a trade-off parameter α was used which ensured appropriate weight on delay spread minimization and filtered noise suppression iteratively. Experimental results show that the method minimized delay spread and noise in optimal sense when compared to other reported techniques. Though delay spread observed is slightly less than that of [6], but [6] does not consider channel noise. Hence, in practical sense, this slight trade-off can be considered profitable with improved SNR and bit rate performance.

Then, to address the issue of spectral nulls in eigenfilter designs, an improved eigenfilter method for TEQ design has been presented. A new objective function was proposed which explicitly attempted to remove the spectral nulls in the frequency response of the shortened channel. Apart from minimizing residual power of SIR and filtered noise power, delay spread minimization of the desired portion of SIR with respect to a suitable time reference were incorporated to ensure that frequency response flattens to remove spectral nulls and hence allows to transmit more data over the useful signal spectrum. Delay dependent matrices in the proposed method could be updated for each transmission delay Δ following the guidelines of [26] which further reduces computational burden. A heuristic choice of optimum transmission delay was proposed which not only allows solving generalized EV problem only once for TEQ design but also yields profitable bit rate performance. Both the proposed methods with and without heuristic choice of delay perform satisfactorily in terms of bit rate which are evident from the simulation results.

Finally, an iterative MSSNR method has been proposed to improve the performance of the direct MSSNR method with reduced delay sensitivity. A step size adaptive algorithm has been derived for faster convergence which can be incorporated to any eigenfilter based channel shortening method. TEQs designed by iterative method tend to introduce less nulls in the shortened channel frequency response. Thus, the proposed method entails significant bit rate improvement along with other computational benefits.

In Chapter 4, a MIMO TEQ design algorithm has been derived for cyclic-prefixed block transmission systems. In literature, most of the TEQ design methods proposed are for SISO channel. MIMO TEQ design has recently received considerable attention. The proposed algorithm has been developed based on maximizing energy within a window of the shortened channel. This method basically extends popular low complexity MSSNR method for SISO channel to MIMO case. Simulation results provided a comparative study of the method with respect to equalization SNR, energy compaction ratio, signal to interference ratio and bit rate was presented with respect to MMSE based method.

5.2 Suggestions for future work

Although a large number of publications has appeared on the topic of time domain equalizer design there is still room for innovation. This dissertation presents several optimal time domain equalizers by taking into account avoidance of spectral nulls, minimization of delay spread and suppression of filtered noise power which performed well for tested ADSL CSA loops no. 1-8.

Most of the TEQ design methods depends on exhaustive search for finding optimum transmission delay. In this regard, a heuristic choice of optimum transmission delay is presented which, though performed well, suffers slight performance loss in bit rate. But, how to find optimum delay on concrete mathematical or analytical basis is still an open problem. Derivation of optimum transmission delay may vary for different TEQ design methods.

The development of the proposed methods assumes that channel state information and noise statistics are present in the receiver. However, in dynamic rapid dispersive channels/environments, this assumption is far from ideal. Hence, blind adaptive channel shortening is of particular interest in this field. Recently, few methods [32], [33], [34] has emerged in the literature that dealt with dynamic channel. As emerging wireline and wireless communication technologies tend to utilize multiuser diversity, multiuser channel shortening [35] is also of utmost importance to attain satisfactory QoS gain.

This dissertation did not include noise sources such as far-end crosstalk (FEXT) or near-end echo to the model of the subchannel SNR. Near-end echo from the local transmitter is a powerful source of noise and it would be worthwhile to

include it in future SNR models.

From the surveyed literature, it is seen that the methods applicable to a single-input single-output TEQ design methods can be adapted to a MIMO system approach. Single-input single-output MMSE method has an equivalent in the multiple-input multiple-output approach. In Chapter 4, popular MSSNR method has been extended to MIMO case, and it is possible that other methods such as MDS, Min-ISI can be adapted as well.

While recent designs have focused on maximizing the bit rate for a given bit error rate in the context of wireline multicarrier systems (such as DSL), wireless multicarrier systems usually have a fixed bit loading, and the receiver performance is measured in terms of bit error rate (BER) for a fixed bit rate. Only one attempt has been reported so far [36] to design TEQ in the context of wireless OFDM systems to improve BER performance. Hence, low complexity TEQ design to improve BER is of significant interest off late.

The simulation results presented in this dissertation treat the performance of the time domain equalization methods in the downstream direction. Upstream section is not simulated; however, it may be of interest to find if the performance of the time domain equalization changes if duplex communication system is incorporated in the simulation set up.

105923

References

- [1] ANSI-T1.413-1995, "Network and customer installation interfaces:asymmetrical digital subscriber line (ADSL) metallic interface," *ADSL Forum System Reference Model*, 1995.
- [2] A. Tkacenko and P. P. Vaidyanathan, "A low-complexity eigenfilter design method for channel shortening equalizers for DMT systems." *IEEE Trans. on Communications*, vol. 51, no. 7, pp. 1069–1072, 2003.
- [3] N. Al-Dhahir and J. M. Cioffi, "Efficiently computed reduced- parameter input-aided MMSE equalizers for ML detection: A unified approach," *IEEE Trans. on Info. Theory*, vol. 42, no. 3, pp. 903–915, 1996.
- [4] P. J. W. Melsa, R. C. Younce, and C. E. Rohrs, "Impulse response shortening for discrete multitone transceivers," *IEEE Trans. on Communications*, vol. 44, no. 12, pp. 1662–1672, 1996.
- [5] R. Schur and J. Speidel, "An efficient equalization method to minimize delay spread in OFDM/DMT systems," in *Proc. of IEEE Int. Conf. Communications*, vol. 5, pp. 1481–1485, 2001 .
- [6] R. L. Valcarce, "Minimum delay spread TEQ design in multicarrier systems," *IEEE Signal Processing Letters*, vol. 11, no. 8, pp. 682–685, 2004.
- [7] J. A. C. Bingham, "Multicarrier modulation for data transmission: An idea whose time has come," *IEEE Communications Magazine*, vol. 28, no. 5, pp. 5–14, 1990.
- [8] ETS-300-401, "Radio broadcast systems; digital audio broadcasting (dab) to mobile, portable and fixed receivers," *European Telecommunications Standards Institute (ETSI)*, 1994.

- [9] ETS-300-744, "Digital broadcasting systems for television, sound and data services; framing structure, channel coding and modulation for digital terrestrial television," *European Telecommunications Standards Institute (ETSI)*, 1997.
- [10] G. H. Golub and C. F. V. Loan, *Matrix computations*. Baltimore, MD, USA: The Johns Hopkins University Press, 1996.
- [11] R. K. Martin, K. Vanbleu, M. Ding, G. Ysebaert, M. Milosevic, B. L. Evans, M. Moonen, and C. R. Johnson, "Unification and evaluation of equalization structures and design algorithms for discrete multitone modulation systems," *IEEE Trans. on Signal Processing*, vol. 53, no. 10, pp. 3880–3894, 2005.
- [12] R. K. Martin, *Blind, adaptive equalization for multicarrier receivers*. Cornell University, Ithaca, NY, USA: Ph.D. dissertation, 2004.
- [13] D. S. Watkins, *Fundamentals of matrix computations*. USA: John Wiley and Sons, 1991.
- [14] D. D. Falconer and F. R. Magee, "Adaptive channel memory truncation for maximum likelihood sequence estimation," *Bell Sys. Tech. Journal*, pp. 1541–1562, 1973.
- [15] K. V. Acker, G. Leus, M. Moonen, O. van de Wiel, and T. Pollet, "Per tone equalization for DMT-based systems," *IEEE Trans. on Communications*, vol. 49, no. 1, pp. 109–119, 2001.
- [16] R. K. Martin, M. Ding, B. L. Evans, and C. R. Johnson, "Infinite length results and design implications for time-domain equalizers," *IEEE Trans. on Signal Processing*, vol. 52, no. 1, pp. 297–301, 2004.
- [17] C. Yin and G. Yue, "Optimal impulse response shortening for discrete multitone transceivers," *Electronics Letters*, vol. 34, no. 1, pp. 35–36, 1998.
- [18] R. K. Martin, C. R. J. Jr., M. Ding, and B. L. Evans, "Exploiting symmetry in channel shortening equalizers," in *Proc. of IEEE Int. Conf. on Acoustics, Speech, and Signal Processing*, vol. 5, no. 4, pp. 97–100, 2003.

- [19] G. Arslan, B. L. Evans, and S. Kiaei, "Equalization for discrete multitone receivers to maximize bit rate," *IEEE Trans. on Signal Processing*, vol. 49, no. 12, pp. 3123–3135, 2001.
- [20] X. Yang, T. K. Sarkar, and E. Arvas, "A survey of conjugate gradient algorithms for solution of extreme eigen-problems of a matrix," in *Proc. of IEEE Int. Conf. on Acoustics, Speech, and Signal Processing*, vol. 37, no. 10, pp. 1550–1556, 1989.
- [21] D. Daly, C. Heneghan, and A. D. Fagan, "A minimum mean-squared error interpretation of residual ISI channel shortening for discrete multitone transceivers," in *Proc. of IEEE Int. Conf. on Acoustics, Speech, and Signal Processing*, vol. 4, no. 5, pp. 2065–2068, 2001.
- [22] S. Celebi, "Interblock interference (IBI) and time of reference (TOR) computation in OFDM systems," *IEEE Trans. on Communications*, vol. 49, no. 11, pp. 1895–1900, 2001.
- [23] I. Ilani, *Time domain equalizer for DMT transceivers - A geometric approach*. USA: US patent 6341298, 2002.
- [24] G. Arslan and M. Ding and B. Lu and M. Milosevic and Z. Shen and B. L. Evans. MATLAB DMTTEQ toolbox 3.1 Beta 3 Release. The University of Texas at Austin. [Online]. Available: <http://www.ece.utexas.edu/~bevans/projects/adsl/dmtteq/dmtteq.html>. July 27, 2003.
- [25] B. Farhang-Bouroujeny and M. Ding, "Design methods for time-domain equalizers in DMT transceivers," *IEEE Trans. on Communications*, vol. 49, no. 3, pp. 554–562, 2001.
- [26] R. K. Martin, M. Ding, B. L. Evans, and C. R. Johnson, "Efficient channel shortening equalizer design," *EURASIP Journal on Applied Signal Processing*, vol. 2003, no. 13, pp. 1279–1290, 2003.
- [27] J. M. Cioffi. "A multicarrier primer". [Online]. Available: <http://wwwisl.stanford.edu/people/cioffi/pdf/multicarrier.pdf>. 2001.

- [28] M. Ding, B. L. Evans, R. K. Martin, and C. R. Johnson, "Minimum inter-symbol interference methods for time domain equalizer design," in *Proc. of IEEE Global. Telecommun. Conf.*, vol. 4, pp. 2146-2150, 2003.
- [29] C. Chatterjee, V. P. Roychowdhury, J. Ramos, and M. D. Zoltowski, "Self-organizing algorithms for generalized eigen-decomposition," *IEEE Trans. on Neural Networks*, vol. 8, no. 6, pp. 1518-1530, 1997.
- [30] N. Al-Dhahir, "FIR channel-shortening equalizers for MIMO ISI channels," *IEEE Trans. on Communications*, vol. 49, no. 2, pp. 213-218, 2001.
- [31] L. Youming, "Maximum shortening SNR design for MIMO channels," in *Proc. of IEEE Int. Symp. Microwave, Antenna, Propagation and EMC Tech. for Wireless Comm.*, vol. 2, pp. 1488-1491, 2005.
- [32] R. K. Martin, J. M. Walsh, and C. R. Johnson, "Low complexity MIMO blind, adaptive channel shortening," *IEEE Trans. on Signal Processing*, vol. 53, no. 4, pp. 1324-1334, 2005.
- [33] H. Kameyama, T. Miyajima, and Z. Ding, "Perfect blind-channel shortening for multicarrier systems," *IEEE Trans. on Circuits and Systems I: Regular Papers*, vol. 55, no. 3, pp. 851-860, 2008.
- [34] R. K. Martin, "Fast-converging blind adaptive channel-shortening and frequency-domain equalization," *IEEE Trans. on Signal Processing*, vol. 55, no. 1, pp. 102-110, 2007.
- [35] R. Samanta, J. R. W. Heath, and B. L. Evans, "Joint interference cancellation and channel shortening in Multiuser-MIMO systems," *IEEE Trans. on Vehicular Technology*, vol. 56, no. 2, pp. 652-660, 2007.
- [36] R. K. Martin, G. Ysebaert, and K. Vanbleu, "Bit error rate minimizing channel shortening equalizers for cyclic prefixed systems," *IEEE Trans. on Signal Processing*, vol. 55, no. 6, pp. 2605-2616, 2007.
- [37] M. H. Hayes, *Statistical digital signal processing and modeling*. NY: Wiley, 1996.

- [38] J. Kim and E. J. Powers, "Subsymbol equalization for discrete multitone systems." *IEEE Trans. on Communications*, vol. 53, no. 9, pp. 1551–1560, 2005.

Appendix A

Analysis of important equations

A.1 Proof of equivalence of equation 4.12 and 4.13

Two cost functions will lead to the same TEQ, except they might be different by a scale factor. However, note that the matrix \mathbf{C} is same for all delays, where as the matrix \mathbf{B} has to be recomputed for each delay. Thus, if we want to run the design over useful range of delays, it is faster not to compute the matrix \mathbf{B} . To see the equivalence, we write the MSSNR design as (for convenience, formulation is shown for SISO systems, which can be easily extended to MIMO systems by incorporating *trace* function as used in 4.12 and 4.13)

$$\begin{aligned} \mathbf{w}_{opt} &= \operatorname{argmin}_{\mathbf{w}} \frac{\mathbf{w}^T \mathbf{A} \mathbf{w}}{\mathbf{w}^T \mathbf{B} \mathbf{w}} \\ &= \operatorname{argmax}_{\mathbf{w}} \frac{\mathbf{w}^T \mathbf{B} \mathbf{w}}{\mathbf{w}^T \mathbf{A} \mathbf{w}} \end{aligned} \quad (\text{A.1})$$

As $\mathbf{C} = \mathbf{A} + \mathbf{B}$, then

$$\begin{aligned} \mathbf{w}_{opt} &= \operatorname{argmax}_{\mathbf{w}} \frac{\mathbf{w}^T (\mathbf{C} - \mathbf{A}) \mathbf{w}}{\mathbf{w}^T \mathbf{A} \mathbf{w}} \\ &= \operatorname{argmax}_{\mathbf{w}} \left[\frac{\mathbf{w}^T \mathbf{C} \mathbf{w}}{\mathbf{w}^T \mathbf{A} \mathbf{w}} - \frac{\mathbf{w}^T \mathbf{A} \mathbf{w}}{\mathbf{w}^T \mathbf{A} \mathbf{w}} \right] \\ &= \operatorname{argmax}_{\mathbf{w}} \left[\frac{\mathbf{w}^T \mathbf{C} \mathbf{w}}{\mathbf{w}^T \mathbf{A} \mathbf{w}} - 1 \right] \\ &= \operatorname{argmax}_{\mathbf{w}} \frac{\mathbf{w}^T \mathbf{C} \mathbf{w}}{\mathbf{w}^T \mathbf{A} \mathbf{w}} \end{aligned} \quad (\text{A.2})$$

$$= \operatorname{argmin}_{\mathbf{w}} \frac{\mathbf{w}^T \mathbf{A} \mathbf{w}}{\mathbf{w}^T \mathbf{C} \mathbf{w}} \quad (\text{A.3})$$

Hence, computing \mathbf{C} outside the loop over delays entails significant computational savings. That way, computing \mathbf{A} only, allows fewer additions/subtractions. The

resulting design may change by an amplitude scale factor from one line to the next, but that does not affect the ratios of $(\mathbf{w}^T \mathbf{B} \mathbf{w} / \mathbf{w}^T \mathbf{A} \mathbf{w})$ or $(\mathbf{w}^T \mathbf{C} \mathbf{w} / \mathbf{w}^T \mathbf{A} \mathbf{w})$.

A.2 Decomposition of generalized EV problem of equation 3.39

\mathbf{Y} is a positive-definite centrosymmetric matrix and can be decomposed by Cholesky decomposition into

$$\begin{aligned} \mathbf{Y} &= \mathbf{Q} \Lambda \mathbf{Q}^T = (\mathbf{Q} \sqrt{\Lambda}) (\sqrt{\Lambda} \mathbf{Q}^T) \\ &= (\mathbf{Q} \sqrt{\Lambda}) (\mathbf{Q} \sqrt{\Lambda})^T = \sqrt{\mathbf{Y}} \sqrt{\mathbf{Y}}^T \end{aligned} \quad (\text{A.4})$$

where Λ is a diagonal matrix formed from the eigenvalues of \mathbf{Y} , and the columns of \mathbf{Q} are the orthonormal eigenvectors. Define

$$\mathbf{Z} = (\sqrt{\mathbf{Y}})^{-1} \mathbf{X} (\sqrt{\mathbf{Y}}^T)^{-1} \quad (\text{A.5})$$

Using a similar development as in [4], the optimal equalizer coefficients for a particular Δ can be given as

$$\mathbf{w}_\Delta = (\sqrt{\mathbf{Y}}^T)^{-1} \mathbf{l}_{min} \quad (\text{A.6})$$

where \mathbf{l}_{min} is the unit length eigenvector corresponding to the minimum eigenvalue λ_{min} of \mathbf{Z} .

Appendix B

Configuration of 8 CSA loop TP channels

In this section, we characterize the TP channels in terms of poles and zeros. Shanks method [37], [38] is used to obtain the poles and zeros of the channels. The channel configurations used for the testing of the ADSL system are investigated.

The poles and the zeros of the eight CSA loops which are the closest and the second closest to the unit circle are listed in Table B.1. Pole # 1 (# 2) and Zero # 1 (# 2) are the closest (second closest) poles and zeros, respectively. The number in the parenthesis beside the complex numbers denotes the corresponding magnitude. Table B.1 shows that every CSA loop contains a pole which is close to the unit circle, resulting in a long channel impulse response. Based on the locations of poles and zeros in Table B.1, it can be concluded that the CSA loops contain a unique dominant pole which is responsible for the long impulse responses, but rarely contain a zero close to the unit circle.

In Fig. B.1, configuration of 8 standard CSA loops are shown with bridge taps at various length. The symbol $x/26$ means the length of x feet of the bridged tap whose size is 26 American Wire Gauge (AWG). Bridged taps refer

Table B.1: Dominant poles and zeros of 8 CSA loops

Channel index	Pole # 1	Pole # 2 (mag)	Zero # 1 (mag)	Zero # 2 (mag)
1	.963	$.596 \pm j.402$ (.719)	-.971	$.693 \pm j.550$ (.885)
2	.964	$.540 \pm j.570$ (.785)	$.752 \pm j.519$ (.914)	.885
3	.968	.695	.861	.859
4	.964	.763	$.781 \pm j.429$ (.891)	.865
5	.967	$-.648 \pm j.479$ (.806)	$.838 \pm j.283$ (.884)	.875
6	.969	.641	$-1.159 \pm j.117$ (.858)	$-1.115 \pm j.347$ (.857)
7	.968	$.676 \pm j.363$ (.768)	$.791 \pm j.459$ (.915)	.904
8	.974	.723	$-1.152 \pm j.094$ (1.156)	.904

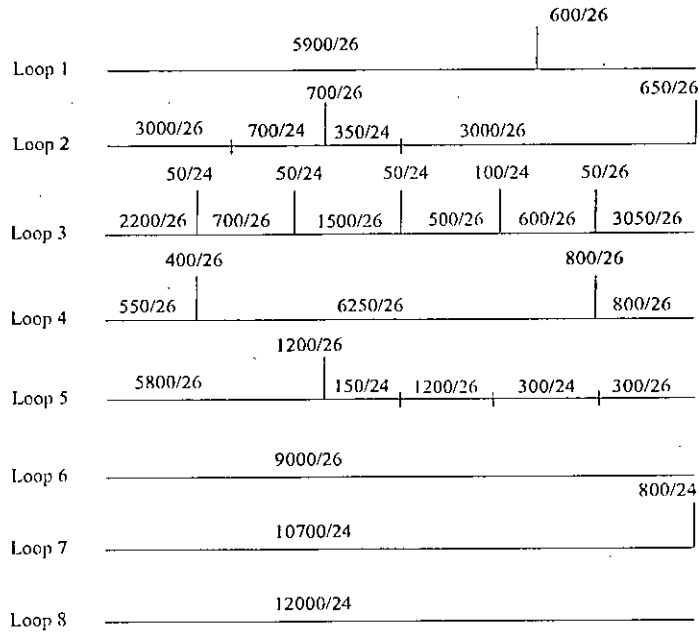


Fig. B.1: Configuration of eight standard CSA loops. Numbers represent length/thickness in feet per gauge. Vertical lines represent bridge taps.

to an unterminated connection of another local loop to a primary local loop, forming a transmission line stub with adverse effects on the line impedance and transfer function. Many loops contain bridged taps, whether in the local loop or customer premises wiring. A length change of the bridged taps alters spectral null locations of the channel frequency response, but still results in moderate depths of the spectral nulls. We can see that the zeros of the channels remain away from the unit circle via pole zero modeling of the channels. Therefore, it can be said that the bridged taps in the CSA loops do not bring zeros close to the unit circle [38].

Appendix C

List of publications

Partial research results of this thesis work are presented in the following papers:

1. Toufiqul Islam and Md. Kamrul Hasan, "On MIMO channel shortening for cyclic-prefixed systems," accepted for presentation in *IEEE International Conference on Wireless Communications, Networking and Mobile Computing (WiCOM)*, China. October 2008.
2. Toufiqul Islam, Md. Shafi Al Bashar, Satya Prasad Majumder and Md. Kamrul Hasan, "Improved eigenfilter design method for channel shortening equalizers for DMT systems," submitted to *IEEE Signal Processing Letters*.
3. Toufiqul Islam, Satya Prasad Majumder and Md. Kamrul Hasan, "Noise optimized minimum delay spread equalizer design for DMT transceivers," accepted for presentation in *International Conference on Electrical and Computer Engineering (ICECE)*, Dhaka. December 2008.
4. Md. Ariful Haque, Toufiqul Islam and Md. Kamrul Hasan, "Speech dereverberation in the noisy condition using delay-and-sum beamforming and channel shortening approach," submitted to *IEEE International Conference on Acoustics, Speech, and Signal Processing (ICASSP)*, Taiwan. April 2009.